

doi:10.3799/dqkx.2017.614

祁连地块西段硫磺矿北花岗闪长岩的岩石成因及其地质意义:年代学、地球化学及 Hf 同位素证据

陶刚¹, 朱利东¹, 李智武^{1,2}, 欧阳慧子¹, 解龙¹, 杨文光¹, 杨珍¹

1. 成都理工大学沉积地质研究院, 四川成都 610059

2. 油气藏地质及开发工程国家重点实验室, 四川成都 610059

摘要: 祁连地区与 Rodinia 超大陆汇聚有关的新元古代岩浆活动越来越受到地质学者的关注和研究。对硫磺矿北花岗闪长岩体进行了锆石 LA-ICP-MS U-Pb 定年, 结果显示岩体锆石 U-Pb 年龄加权平均值为 926 ± 4 Ma, 表明其形成时代新元古代早期。花岗闪长岩的 SiO_2 为 59.47%~62.96%, P_2O_5 为 0.12%~0.14%, 铝饱和指数(A/CNK)为 1.01~1.15, 主要为一套弱过铝质的高钾钙碱型系列, 具 I 型花岗岩的特征。稀土元素总量在 118.80×10^{-6} ~ 253.07×10^{-6} 之间, $(\text{La}/\text{Yb})_N$ 为 7.87~16.17, 明显富集轻稀土, 具有中等一强 Eu 负异常($\delta\text{Eu}=0.33\sim 0.68$), 稀土元素配分图呈右倾型特征; 微量元素上具有富集大离子亲石元素和不相容元素(Rb、Th 和 U), 亏损高场强元素 Nb、Ta、Ti、Sr 和 P 的特征; Nb/Ta、La/Nb、Nb/U 及 Sm/Nd 比值整体反映花岗闪长岩壳源特点; 硫磺矿北花岗闪长岩体 $\epsilon_{\text{Hf}}(t)$ 主要在 0~7 之间, 二阶段地壳模式年龄主要在 1 247~1 801 Ma 之间。结合区域新元古代岩浆活动认为硫磺矿北花岗闪长岩体形成于活动大陆边缘, 而硫磺矿北花岗闪长岩为中元古代增生的年轻地壳部分熔融的产物, 经历一定程度分离结晶, 可能也有古老地壳部分熔融成分参与该岩体形成。同时, 该时期岩浆活动可能为祁连地块在中元古代时期对全球 Rodinia 超大陆聚合事件的响应, 进一步为祁连地块属性提供可信研究资料。

关键词: 祁连地块; 花岗闪长岩; 锆石 U-Pb 年龄; Lu-Hf 同位素; 新生地壳; 罗迪尼亚超大陆; 地球化学。

中图分类号: P597

文章编号: 1000-2383(2017)12-2258-18

收稿日期: 2017-03-15

Petrogenesis and Geological Significance of the North Liuhuangkuang Granodiorite in the West Sement of the Qilian Terrane: Evidences from Geochronology, Geochemistry, and Hf Isotopes

Tao Gang¹, Zhu Lidong¹, Li Zhiwu^{1,2}, Ouyang Huizi¹, Xie Long¹, Yang Wenguang¹, Yang Zhen¹

1. Institute of Sedimentary Geology, Chengdu University of Technology, Chengdu 610059, China

2. State Key Laboratory of Oil and Gas Reservoir Geology and Exploitation, Chengdu University of Technology, Chengdu 610059, China

Abstract: More geological researchers are focusing on the Neoproterozoic magmatic activities of Qilian Terrane and little chronological and geochemical materials are about the North Liuhuangkuang Granodiorites (NLG) in the western segment of Qilian Terrane. The zircons of rock samples which had distinct rhythmic growth zoning are long cylindrical and euhedral well, implying the features of magmatic origin. The results of dating indicate that the rocks were formed in the Early Neoproterozoic (926 ± 4 Ma). 11 samples' new whole-rock geochemical analysis results have SiO_2 content of 59.47%~62.96%, P_2O_5 content of 0.12%~0.14% with A/CNK values of 1.01~1.15, which showed that the NLG were high-K calc-alkaline with characteristics of I-type. The ΣREE content was between 118.80×10^{-6} and 253.07×10^{-6} , with $(\text{La}/\text{Yb})_N$ ratio of 7.87~16.17 and δEu (0.89~1.03). The REE diagram showed rightward incline and mid-negative weakly negative Eu abnormality. The NLG were en-

基金项目: 冈底斯-喜马拉雅铜矿资源基地调查项目(No.DD20160015); 中国地质调查项目(No.12120113033004); 高等学校博士学科点专项科研基金资助项目(No.20125122110010)。

作者简介: 陶刚(1988-), 男, 博士研究生, 主要从事青藏高原区域地质及古生物学方面研究。ORCID: 0000-0003-4946-5071。

E-mail: taogang0428@163.com

引用格式: 陶刚, 朱利东, 李智武, 等, 2017. 祁连地块西段硫磺矿北花岗闪长岩的岩石成因及其地质意义: 年代学、地球化学及 Hf 同位素证据. 地球科学, 42(12): 2258-2275.

riched in large-ion lithophile elements: Rb, Th, U, LREE and depleted in high field strength elements: Nb, Ta, Ti, P. The ratios of Nb/Ta, La/Nb, Nb/U and Sm/Nd show crustal characteristics. The Hf isotopes showed that the $\epsilon_{\text{Hf}}(t)$ of NLG mainly ranged from 0 to 7 and its crustal model ages were between 1 247 Ma and 1 801 Ma. With the regional magmatic activities, the NLG probably were formed in a subduction tectonic environment of continental margin arc and it suggested that the primary magma was derived from the remelting of juvenile crustal materials in Mesoproterozoic, experiencing a certain extent of fractional crystallization. Otherwise, the melting of the ancient crust also probably participated the formation of the NLG. The NLG magma activities may be the response of the converge of the Rodinia Supercontinental, during the Neoproterozoic, which provided the attribute of the Qilian Terrane with credible research materials.

Key words: Qilian Terrane; Granodiorite; zircon U-Pb dating; Lu-Hf isotope; juvenile crust; The Rodinia Supercontinental; geochemistry.

祁连地块位于青藏高原东北缘, 夹持于华南地块、华北克拉通和塔里木克拉通之间, 并蕴含着丰富

的古板块构造演化信息, 是研究中国板块构造及其演化历史的关键地区之一(图 1a; 夏林圻等, 2016)。

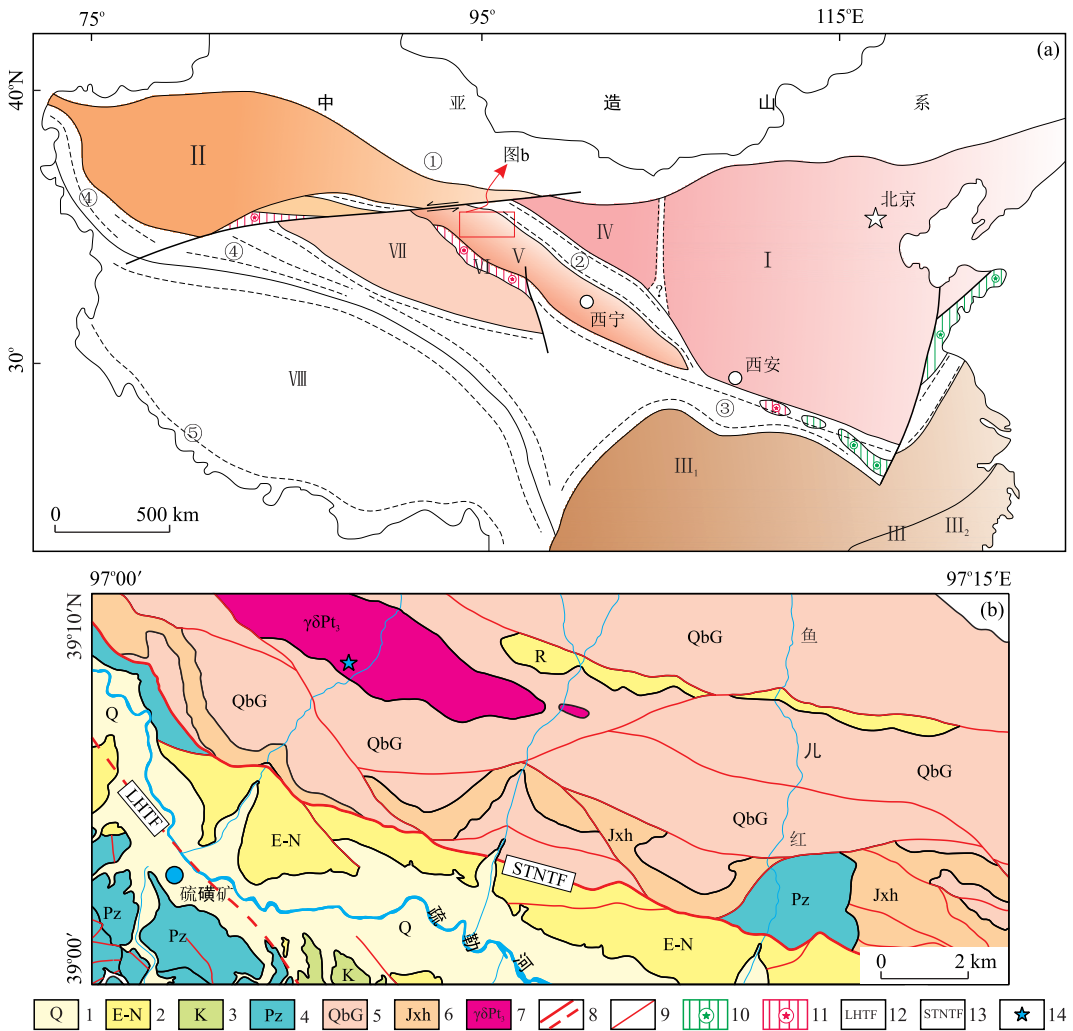


图 1 祁连地块及邻区构造单元图(a)和硫磺矿北地区地质图(b)

Fig.1 Map of tectonic units for the Qilian block and adjacent areas (a) and geological map of the north Liuhuanguang, Western Qilian (b)

图 a 据夏林圻等(2016)修改; 代号: I. 华北克拉通; II. 塔里木克拉通; III. 华南地块; III₁. 扬子地块; III₂. 华夏地块; IV. 阿拉善地块; V. 祁连地块; VI. 柴北缘超高压变质带; VII. 柴达木地块 VIII—青藏高原; 编号: ①. 中亚造山带; ②. 北祁连造山带; ③. 秦岭—大别造山带; ④. 昆仑造山带; ⑤. 喜马拉雅造山带. 图 b1. 第四系; 2. 新近系; 3. 白垩系; 4. 古生界; 5. 龚岔群; 6. 花儿地组; 7. 花岗岩闪长岩; 8. 逆冲断裂; 9. 断层; 10. 三叠纪高压—超高压变质带; 11. 早古生代高压—超高压变质带; 12. 硫磺矿—河淌逆冲断裂; 13. 托莱南山南缘逆冲断裂; 14. 采样位置

80 年代以来,众多学者对于祁连地块寒武纪以来地质体做了大量研究工作,包括蛇绿岩发现和研究(郭原生,1993;冯益民和何世平,1995;张旗等,1998;张招崇等,1998;钱青等,1999;黄增保等,2016)、沉积盆地物源及演化分析(杜远生等,2006;裴先治等,2012;徐亚军等,2013;姜高磊等,2014)、高压-超高压变质岩(Zhang *et al.*, 2009;张建新等,2010;宋述光等,2013)、大量早古生代岩浆岩(吴才来等,2005;雍拥等,2008;李建锋等,2010;秦海鹏等,2014a, 2014b;张照伟等,2015;Yang *et al.*, 2015;Wang *et al.*, 2017),据此也提出各种构造演化模式(许志琴等,1994;Xiao *et al.*, 2009;宋述光等,2013),但是前人对于祁连地块前寒武系研究相对滞后。随着锆石高精度测年技术的不断发展,新涌出了一批可靠的年代学数据资料,对于祁连地块内部前寒武系研究已经成为目前研究热点之一(万渝生等,2003;董国安等,2007;Tung *et al.*, 2013, 2016)。

大量的与罗迪尼亚超大陆(Rodinia)汇聚、拼合作用相关的中-新元古代时期岩浆活动和变质作用事件在中国大陆被识别出来(Chen *et al.*, 1991;Greentree *et al.*, 2006;Li *et al.*, 2007, 2013;Lu *et al.*, 2008;Song *et al.*, 2012, 2013;Yu *et al.*, 2013),主要的响应地块有:华南地块、塔里木地块、阿拉善地块和柴达木地块(Chen *et al.*, 1991;Greentree *et al.*, 2006;Li *et al.*, 2007, 2013;Lu *et al.*, 2008;Shu *et al.*, 2011;Song *et al.*, 2012;Yu *et al.*, 2013;He *et al.*, 2014;Xu *et al.*, 2015;Zhang *et al.*, 2015, 2017, 2016;Wen *et al.*, 2017),同时包括祁连地块,而华北地块内目前未有确信的与 Rodinia 超大陆聚合事件有关的年代学资料(Liu *et al.*, 2013;Xu *et al.*, 2013)。祁连地块新元古代早期构造演化史一直是地质学家关注的焦点,但是,由于早古生代造山和青藏高原隆升作用强烈的构造叠加和造山带隆升剥蚀,导致新元古代早期的大量地质记录被“掩盖”或“丢失”,从而严重制约了我们进一步认识祁连地块新元古代早期地质过程。近年来,随着祁连地块元古宙岩浆活动发现和前寒武系变质基底研究,为深入探讨祁连地块在新元古代时期的构造属性提供了基础地质资料(郭进京等,1999;Gehrels *et al.*, 2003;万渝生等,2003;董国安等,2007;王洪亮等,2007;Tung *et al.*, 2013),同时,新元古代岩浆活动研究已经开始使得关于祁连地块属性和来源的传统认识开始面临挑战:传统观点认为祁连地块为华北板块不同程度裂解“开-合构造”演化,

即北祁连和中祁连发生大陆裂解后,裂隙逐渐向南迁移,进而引起南祁连与中祁连的分离,进一步发育成洋盆,而后又与中祁连发生俯冲-碰撞完成拼合(左国朝和刘寄陈,1987;冯益民等,1996);另一种新的观点认为祁连地块与扬子地块有较强的亲缘性,在新元古代时应同属于冈瓦纳大陆一部分(万渝生等,2003;董国安等,2007;徐旺春等,2007;Tung *et al.*, 2013)。

研究区硫磺矿北岩体分布在祁连地块西段(图 1a),关于其形成时代一直存在不同的认识,1:20 万硫磺山幅认为其侵入于震旦系地层中,将其归入早古生代晚期;青海省区域地质志中认为其侵入于下元古界变质岩,将其划归到前寒武纪(青海省地矿局,1991),造成这种差异性认识的原因在于缺乏精确的年代学和地球化学等方面研究资料。本次研究通过锆石 U-Pb 测年工作发现该岩体产出时代为新元古代,这为研究祁连地块在新元古代时期构造演化研究提供了契机。本文在岩石学基础上对硫磺矿北岩体开展了较为详细的锆石 U-Pb 年代学、Hf 同位素和地球化学等测试工作,研究其岩石成因、岩浆源区性质等,并分析探讨硫磺矿北岩体形成大地构造背景,可为祁连地块在新元古代时期属性提供可信的研究资料。

1 区域地质背景及样品特征

祁连地块北邻北祁连造山带,南接柴北缘超高压变质带,东连西秦岭造山带,向西被阿尔金断裂带截切,并具有古元古代结晶基底、中元古代变质基底、新元古代-古生代沉积盖层(郭进京等,1999;万渝生等,2003;夏林圻等,2016)。研究区内以托莱南山南缘逆冲断裂(STNTF)和硫磺山-河湟逆冲断裂(LHTF)为主线,STNTF 北侧地层沿该断层南向逆冲,LHTF 南侧地层沿该断层北向逆冲,两侧地层形成“对冲”构造样式,后期受喜山期北东-南西向构造影响,使得研究区前寒武纪地层多呈断块状展布(图 1b)。

研究区硫磺矿北岩体空间展布特征受区域构造影响,主要呈北西-南东向展布,岩体以长条状岩株形式产出,出露面积约 10 km²,长轴方向为北西向(图 1b),侵入于新元古代龚岔群并使之发生绿泥石化和黄铁矿化,围岩地层主要有蓟县系花儿地组(Jxh),青白口系龚岔群(QbG),其中龚岔群岩性主要为一套低绿片岩相的陆源碎屑岩和碳酸盐岩,产叠层石和微古植物化石,叠层石时代为新元古代青

白口纪(钱家骥等,1986),与下伏花儿地组(Jxh)平行不整合接触;花儿地组(Jxh)在区域上为一套碳酸盐岩为主体的岩石组合,垂向上具有白云岩—颗粒灰岩—颗粒灰岩夹碎屑岩的垂向序列,反映了沉积环境相对稳定的特征。另外,研究区地层可见古生界、中生界和古近系—新近系,其中,古生代的地层记录了“拉脊山—党河南山洋”在研究区洋陆过程,主要为深海盆地背景下的硅泥质岩→陆缘海环境下的细复理石→陆相快速堆积环境下的粗碎屑岩;白垩系主要为一套紫红色—灰绿色河流—湖泊相沉积碎屑岩;新近系主要以棕红色碎屑岩为主,碎屑粒度具有从下到上由粗变细特点。

2 样品描述及分析方法

本次研究的样品采集于硫磺矿北岩体南侧边部的露头,采样过程中尽可能在岩体不同部位采集,采样点及采样编号为 D2864(39°09′19″N,97°04′43″E)。硫磺矿岩体岩性主要为花岗闪长岩,岩石具块状构造,细粒花岗结构,矿物成分以斜长石(60%)、钾长石(15%)和石英(20%)为主,次要矿物为角闪石(5%)和黑云母(<2%),金属矿物和副矿物少见,含量低于 1%。斜长石主要为更—中长石,呈半自形板状,可见绢云母和绿帘石等蚀变,钾长石为正长石,呈它形粒状,部分蚀变为绢云母,石英为它形粒状,个别晶体包含斜长石,形成包含结构,部分充填于长石晶体之间,角闪石为普通角闪石,呈半自形柱状;黑云母为片状,呈残余状分布,金属矿物主要为褐铁矿,副矿物包含磷灰石和锆石等。

样品锆石分离在河北省廊坊地质调查研究院选矿实验室进行。样品经压碎和淘洗后,使用标准重液和磁性分离技术提取锆石。然后在双目镜下挑选出晶形较好的锆石颗粒,并将挑选出的锆石颗粒粘在双面胶上,随后注入环氧树脂。为了揭露锆石颗粒内部特征和用于 U-Pb 定年,将固定在环氧树脂上的锆石颗粒抛光至原颗粒大小的一半。锆石阴极发光(CL)成像在北京地时科技有限公司完成。

锆石 U-Pb 同位素定年分析在中国地质科学院矿产资源研究所国土资源部成矿作用与资源评价重点实验室完成,所用仪器为 Thermo Finnigan Neptune 型多接收等离子质谱(MC-ICP-MS)仪和与之配套的 Newwave UP213 紫外激光剥蚀系统。激光剥蚀过程中采取单点剥蚀的方式,激光剥蚀斑束直径为 25 μm,频率为 10 Hz,能量密度约为 2.5 J/cm²,

采用氦气作为载气,测试过程中每测定 10 颗锆石前后重复测定 1 个玻璃标准 NIST SRM610、2 个锆石标准 GJ-1 和 1 个锆石标准 Plesovice。锆石 U-Pb 定年和微量元素含量采用 GJ-1 和 NIST SRM610 作为外标分别进行同位素和微量元素分馏校正,Plesovice 用于观察仪器的状态和测试的重现性。详细分析过程参见(侯可军等,2009)。数据处理采用 ICPMSDataCal 软件(Liu *et al.*, 2010),锆石 U-Pb 年龄计算及谐和图的绘制采用 Isoplot 3.0 完成。单个测试数据的误差为 1σ,对于 ²⁰⁶Pb/²³⁸U 年龄大于 1 000 Ma 的锆石采用 ²⁰⁷Pb/²⁰⁶Pb 年龄,否则采用 ²⁰⁶Pb/²³⁸U 年龄。测试结果见表 1。

本研究中锆石微区原位 Lu-Hf 同位素分析在西北大学大陆动力学国家重点实验室进行。激光剥蚀系统是 193 nm 准分子激光剥蚀系统(RESOLUTION M-50, ASI),包含一台 193 nm ArF 准分子激光器,一个双室样品室和电脑控制的高精度 X-Y 样品台移动、定位系统。激光能量密度为 6 J/cm²,频率为 5 Hz,斑束为 44 μm,载气为高纯氦气,为 280 mL/min, Lu-Hf 同位素分析采用多接收等离子体质谱(Nu Plasma II MC-ICPMS)。Lu-Hf 同位素分馏校正采用指数法则计算,采用 ¹⁷⁶Lu/¹⁷⁵Lu = 0.026 56 和 ¹⁷⁶Yb/¹⁷³Yb = 0.786 96 比值扣除 ¹⁷⁶Lu 和 ¹⁷⁶Yb 对 ¹⁷⁶Hf 的干扰,获得准确的 ¹⁷⁶Hf 信号值。Hf 和 Lu 同位素比值采用 ¹⁷⁹Hf/¹⁷⁷Hf = 0.732 50 进行仪器质量歧视效应校正, Yb 同位素比值采用 ¹⁷³Yb/¹⁷¹Yb = 1.123 46 进行仪器质量歧视效应校正。在分析过程中,国际标准锆石样品 91500 和 Mudtank 作为监控样品,详细的分析方法参考文献(Yuan *et al.*, 2008)。锆石 Hf 同位素特征值计算所涉及参数主要为:¹⁷⁶Lu 衰变常数 λ = 1.867 × 10⁻¹¹ a⁻¹(Söderlund *et al.*, 2004)。亏损地幔 DM 的 ¹⁷⁶Lu/¹⁷⁷Hf = 0.038 40, ¹⁷⁶Hf/¹⁷⁷Hf = 0.283 25; 球粒陨石 CHUR 的 ¹⁷⁶Lu/¹⁷⁷Hf = 0.033 2, ¹⁷⁶Hf/¹⁷⁷Hf = 0.282 772(Blichert-Toft *et al.*, 1997); 大陆平均地壳 CC 的 ¹⁷⁶Lu/¹⁷⁷Hf = 0.015, $f_{Lu/Hf}$ 值为 -0.55(Griffin *et al.*, 2002)。测试结果见表 2。

全岩地球化学分析在广州地球化学研究所同位素地球化学实验室完成。主量元素分析采用碱熔法制成玻璃饼,使用 Rigaku 100e 型 X 射线荧光光谱仪(XRF)进行分析,分析精度优于 2%。微量元素使用 Perkin-Elmer Elan 6000 型电感耦合等离子体质谱仪(ICP-MS)分析,样品中微量元素含量大于 10 × 10⁻⁶ 的分析精度优于 5%,小于 10 × 10⁻⁶ 的分

表 1 祁连山段硫磺矿北花岗岩长岩锆石 LA-MC-ICP-MS U-Pb 年龄数据
 Table 1 LA-MC-ICP-MS U-Pb data of zircon for granodiorites in northern Lihuanguang, Western Qilian

| 编号 | Pb (10^{-6}) | Th (10^{-6}) | U (10^{-6}) | Th/U | 比值 | | | | 年龄 (Ma) | | | | 谐和度 (%) | | | | |
|----|---------------------|---------------------|--------------------|------|----------------------------------|-----------|-----------------------------------|-----------|----------------------------------|-----------|----------------------------------|-----------|------------|-----------------------------------|-----------|----------------------------------|-----------|
| | | | | | $^{207}\text{Pb}/^{235}\text{U}$ | 1σ | $^{207}\text{Pb}/^{206}\text{Pb}$ | 1σ | $^{206}\text{Pb}/^{238}\text{U}$ | 1σ | $^{207}\text{Pb}/^{235}\text{U}$ | 1σ | | $^{207}\text{Pb}/^{206}\text{Pb}$ | 1σ | $^{206}\text{Pb}/^{238}\text{U}$ | 1σ |
| 1 | 131.8 | 191.4 | 858.5 | 0.22 | 1.5183 | 0.0242 | 0.0707 | 0.0011 | 0.1553 | 0.0012 | 938 | 10 | 950 | 33 | 931 | 7 | 99 |
| 2 | 98.0 | 170.1 | 636.2 | 0.27 | 1.5177 | 0.0311 | 0.0713 | 0.0016 | 0.1546 | 0.0020 | 938 | 13 | 969 | 46 | 927 | 11 | 98 |
| 3 | 69.5 | 119.0 | 446.4 | 0.27 | 1.4925 | 0.0271 | 0.0700 | 0.0013 | 0.1546 | 0.0014 | 927 | 11 | 928 | 39 | 927 | 8 | 99 |
| 4 | 60.9 | 96.9 | 392.9 | 0.25 | 1.4848 | 0.0334 | 0.0704 | 0.0018 | 0.1536 | 0.0018 | 924 | 14 | 939 | 52 | 921 | 10 | 99 |
| 5 | 66.1 | 110.8 | 426.7 | 0.26 | 1.4712 | 0.0367 | 0.0696 | 0.0017 | 0.1532 | 0.0018 | 919 | 15 | 917 | 50 | 919 | 10 | 99 |
| 6 | 97.9 | 231.0 | 599.2 | 0.39 | 1.5118 | 0.0506 | 0.0704 | 0.0022 | 0.1551 | 0.0022 | 935 | 20 | 943 | 65 | 930 | 12 | 99 |
| 7 | 89.9 | 128.0 | 583.3 | 0.22 | 1.4890 | 0.0230 | 0.0712 | 0.0011 | 0.1518 | 0.0010 | 926 | 9 | 962 | 31 | 911 | 6 | 98 |
| 8 | 75.1 | 116.7 | 485.7 | 0.24 | 1.4606 | 0.0407 | 0.0695 | 0.0018 | 0.1523 | 0.0016 | 914 | 17 | 922 | 56 | 914 | 9 | 99 |
| 9 | 91.5 | 224.9 | 553.4 | 0.41 | 1.5570 | 0.0471 | 0.0730 | 0.0021 | 0.1543 | 0.0018 | 953 | 19 | 1017 | 53 | 925 | 10 | 96 |
| 10 | 86.2 | 112.2 | 554.5 | 0.20 | 1.5128 | 0.0288 | 0.0713 | 0.0013 | 0.1539 | 0.0013 | 936 | 12 | 969 | 39 | 923 | 7 | 98 |
| 11 | 75.9 | 184.3 | 447.8 | 0.41 | 1.5307 | 0.0314 | 0.0705 | 0.0015 | 0.1574 | 0.0013 | 943 | 13 | 943 | 43 | 942 | 7 | 99 |
| 12 | 76.2 | 145.7 | 462.7 | 0.31 | 1.5179 | 0.0300 | 0.0706 | 0.0014 | 0.1559 | 0.0012 | 938 | 12 | 946 | 42 | 934 | 7 | 99 |
| 13 | 139.7 | 325.1 | 839.2 | 0.39 | 1.5141 | 0.0472 | 0.0705 | 0.0028 | 0.1562 | 0.0028 | 936 | 19 | 944 | 86 | 936 | 15 | 99 |
| 14 | 81.9 | 140.1 | 497.2 | 0.28 | 1.5520 | 0.0356 | 0.0711 | 0.0017 | 0.1578 | 0.0015 | 951 | 14 | 961 | 44 | 945 | 8 | 99 |
| 15 | 188.1 | 450.6 | 1721.2 | 0.26 | 0.9866 | 0.0168 | 0.0670 | 0.0011 | 0.1065 | 0.0009 | 697 | 9 | 839 | -164 | 652 | 5 | 93 |
| 16 | 64.8 | 141.4 | 392.7 | 0.36 | 1.5108 | 0.0335 | 0.0705 | 0.0017 | 0.1557 | 0.0016 | 935 | 14 | 943 | 49 | 933 | 9 | 99 |
| 17 | 68.7 | 140.9 | 422.0 | 0.33 | 1.5078 | 0.0289 | 0.0703 | 0.0013 | 0.1547 | 0.0012 | 934 | 12 | 939 | 39 | 927 | 7 | 99 |
| 18 | 127.4 | 187.0 | 807.0 | 0.23 | 1.4984 | 0.0487 | 0.0703 | 0.0021 | 0.1533 | 0.0026 | 929 | 20 | 939 | 60 | 920 | 15 | 98 |
| 19 | 77.0 | 193.1 | 466.2 | 0.41 | 1.5052 | 0.0403 | 0.0702 | 0.0020 | 0.1550 | 0.0019 | 932 | 16 | 1000 | 57 | 929 | 10 | 99 |
| 20 | 84.6 | 115.4 | 532.4 | 0.22 | 1.5024 | 0.0372 | 0.0703 | 0.0017 | 0.1539 | 0.0016 | 904 | 15 | 937 | 49 | 923 | 9 | 99 |
| 21 | 86.3 | 160.9 | 538.0 | 0.30 | 1.4888 | 0.0776 | 0.0709 | 0.0037 | 0.1511 | 0.0031 | 902 | 32 | 954 | 107 | 907 | 17 | 97 |
| 22 | 81.9 | 128.4 | 504.1 | 0.25 | 1.5107 | 0.0288 | 0.0702 | 0.0014 | 0.1551 | 0.0014 | 900 | 12 | 1000 | 39 | 929 | 8 | 99 |
| 23 | 74.4 | 141.8 | 454.8 | 0.31 | 1.5540 | 0.0381 | 0.0731 | 0.0019 | 0.1533 | 0.0019 | 952 | 15 | 1017 | 52 | 920 | 11 | 96 |
| 24 | 158.7 | 255.3 | 1005.5 | 0.25 | 1.4386 | 0.0410 | 0.0686 | 0.0019 | 0.1507 | 0.0022 | 905 | 17 | 887 | 57 | 905 | 12 | 99 |
| 25 | 111.3 | 205.4 | 684.0 | 0.30 | 1.4888 | 0.0338 | 0.0697 | 0.0016 | 0.1536 | 0.0015 | 926 | 14 | 918 | 46 | 921 | 8 | 99 |

表 2 祁连西段硫磺矿北花岗闪长岩的锆石 LA-MC-ICP-MS Lu-Hf 同位素数据

Table 2 LA-MC-ICP-MS Lu-Hf isotope data of zircon for granodiorites in northern Liuhuangkuang, Western Qilian

| 编号 | t (Ma) | $^{176}\text{Yb}/^{177}\text{Hf}$ | 2σ | $^{176}\text{Lu}/^{177}\text{Hf}$ | 2σ | $^{176}\text{Hf}/^{177}\text{Hf}$ | 2σ | $^{176}\text{Hf}/^{177}\text{Hf}(t)$ | $\epsilon_{\text{Hf}}(t)$ | T_{DM1} (Ma) | T_{DM2} (Ma) | $f_{\text{Lu/Hf}}$ |
|----|----------|-----------------------------------|-----------|-----------------------------------|-----------|-----------------------------------|-----------|--------------------------------------|---------------------------|-----------------------|-----------------------|--------------------|
| 1 | 931 | 0.031 756 | 0.000 394 | 0.001 135 | 0.000 014 | 0.282 303 | 0.000 022 | 0.282 283 | 3.3 | 1 346 | 1 589 | -0.97 |
| 2 | 927 | 0.043 508 | 0.000 489 | 0.001 574 | 0.000 010 | 0.282 348 | 0.000 021 | 0.282 321 | 4.5 | 1 297 | 1 508 | -0.95 |
| 3 | 927 | 0.059 008 | 0.000 386 | 0.002 047 | 0.000 012 | 0.282 439 | 0.000 020 | 0.282 404 | 7.5 | 1 182 | 1 322 | -0.94 |
| 4 | 921 | 0.019 916 | 0.000 462 | 0.000 914 | 0.000 010 | 0.282 169 | 0.000 017 | 0.282 153 | -1.5 | 1 524 | 1 883 | -0.97 |
| 5 | 919 | 0.027 673 | 0.000 294 | 0.000 985 | 0.000 011 | 0.282 135 | 0.000 027 | 0.282 118 | -2.9 | 1 575 | 1 963 | -0.97 |
| 6 | 930 | 0.044 947 | 0.000 471 | 0.001 572 | 0.000 006 | 0.282 317 | 0.000 019 | 0.282 290 | 3.5 | 1 341 | 1 575 | -0.95 |
| 7 | 911 | 0.009 521 | 0.000 207 | 0.000 354 | 0.000 009 | 0.282 194 | 0.000 018 | 0.282 188 | -0.6 | 1 468 | 1 813 | -0.99 |
| 8 | 914 | 0.037 783 | 0.000 387 | 0.001 365 | 0.000 019 | 0.282 352 | 0.000 022 | 0.282 329 | 4.5 | 1 284 | 1 497 | -0.96 |
| 9 | 925 | 0.029 272 | 0.000 508 | 0.001 041 | 0.000 010 | 0.282 282 | 0.000 022 | 0.282 264 | 2.5 | 1 371 | 1 634 | -0.97 |
| 10 | 923 | 0.023 153 | 0.000 378 | 0.000 916 | 0.000 008 | 0.282 057 | 0.000 019 | 0.282 041 | -5.5 | 1 681 | 2 131 | -0.97 |
| 11 | 942 | 0.036 032 | 0.000 679 | 0.001 293 | 0.000 016 | 0.282 381 | 0.000 025 | 0.282 358 | 6.2 | 1 242 | 1 415 | -0.96 |
| 12 | 934 | 0.024 153 | 0.000 567 | 0.000 883 | 0.000 014 | 0.282 202 | 0.000 022 | 0.282 187 | -0.1 | 1 477 | 1 801 | -0.97 |
| 13 | 936 | 0.036 604 | 0.000 848 | 0.001 309 | 0.000 019 | 0.282 263 | 0.000 024 | 0.282 240 | 1.9 | 1 408 | 1 681 | -0.96 |
| 14 | 945 | 0.081 255 | 0.002 073 | 0.002 986 | 0.000 063 | 0.282 486 | 0.000 028 | 0.282 432 | 8.9 | 1 145 | 1 247 | -0.91 |
| 16 | 933 | 0.029 120 | 0.000 360 | 0.001 069 | 0.000 004 | 0.282 341 | 0.000 020 | 0.282 322 | 4.7 | 1 290 | 1 500 | -0.97 |
| 17 | 927 | 0.025 779 | 0.000 569 | 0.000 937 | 0.000 016 | 0.282 254 | 0.000 017 | 0.282 237 | 1.6 | 1 407 | 1 692 | -0.97 |
| 18 | 920 | 0.026 204 | 0.000 723 | 0.000 931 | 0.000 017 | 0.282 230 | 0.000 019 | 0.282 214 | 0.6 | 1 440 | 1 750 | -0.97 |
| 19 | 929 | 0.015 205 | 0.000 435 | 0.000 549 | 0.000 017 | 0.282 239 | 0.000 020 | 0.282 229 | 1.3 | 1 414 | 1 709 | -0.98 |
| 20 | 923 | 0.036 767 | 0.001 013 | 0.001 292 | 0.000 029 | 0.282 332 | 0.000 020 | 0.282 310 | 4.0 | 1 310 | 1 534 | -0.96 |
| 21 | 907 | 0.019 698 | 0.000 498 | 0.000 703 | 0.000 013 | 0.281 912 | 0.000 033 | 0.281 900 | -10.8 | 1 870 | 2 451 | -0.98 |
| 22 | 929 | 0.060 901 | 0.001 781 | 0.002 147 | 0.000 052 | 0.282 428 | 0.000 024 | 0.282 391 | 7.1 | 1 202 | 1 349 | -0.94 |
| 23 | 920 | 0.026 854 | 0.000 315 | 0.000 979 | 0.000 017 | 0.282 284 | 0.000 022 | 0.282 267 | 2.5 | 1 367 | 1 631 | -0.97 |
| 24 | 905 | 0.039 007 | 0.001 025 | 0.001 370 | 0.000 028 | 0.282 335 | 0.000 026 | 0.282 311 | 3.7 | 1 309 | 1 542 | -0.96 |
| 25 | 921 | 0.018 796 | 0.000 397 | 0.000 668 | 0.000 014 | 0.282 072 | 0.000 023 | 0.282 060 | -4.8 | 1 649 | 2 089 | -0.98 |

析精度优于 10%，所有稀土元素的分析精度优于 5%。详细的分析流程和相关参数见(刘颖等, 1996)，分析结果见表 3。

3 分析结果

3.1 锆石 U-Pb 测年结果

通过详细分析对比锆石的透反射、阴极发光照片,选择晶形相似、晶体形态完整、内部结构清晰且振荡环带发育的长柱状自形锆石颗粒,在无裂隙或杂质的干净边部进行打点测试。锆石 LA-ICPMS U-Pb 测点阴极发光图像见图 2a, U-Th-Pb 同位素分析结果见表 1, 锆石谐和图 2b。普遍认为锆石 Th/U 比值在一定程度上能够指示锆石成因环境, 岩浆成因锆石多具有特征性的韵律环带, Th、U 含量较高, 且 Th/U 比值一般大于 0.1, 而变质锆石则表现出无环带、弱环带、低 Th/U 比值(一般小于 0.1)特征(Simon and Nigel, 2007)。

样品 D2864-N 的锆石颗粒主要为自形棱柱状晶体, 长 100~170 μm , 长宽比一般在 2:1~3:1 之间。在 CL 图像上, 锆石颗粒呈现出明显的岩浆振

荡环带, 少数锆石颗粒具有变质增生边(图 2a), 25 个测点数据见表 2。在去除由于不同程度 Pb 丢失造成明显不谐和年龄数据、成因难以解释或混合年龄的测点数据后, 对剩余数据处理计算。25 个测点分析产生的 Th/U 比值为 0.20~0.41, 表明锆石均为岩浆成因, 并获得了 $652 \pm 5 \text{ Ma} \sim 945 \pm 8 \text{ Ma}$ 的 $^{206}\text{Pb}/^{238}\text{U}$ 年龄(表 1)。测试年龄数据大多位于谐和线上或紧邻谐和线, 其中测点 15 具有明显年轻的 $^{206}\text{Pb}/^{238}\text{U}$ 年龄($652 \pm 5 \text{ Ma}$), 可能为 Pb 丢失所致, 其余 24 个测点的加权平均年龄为 $926 \pm 4 \text{ Ma}$ (图 2b), 该年龄代表了硫磺矿北花岗闪长岩的结晶年龄, 为新元古代早期。

3.2 锆石 Lu-Hf 同位素测试结果

硫磺矿北岩体(D2864-N)的锆石 Hf 同位素测点的阴极发光图像见图 2a, 24 个测点锆石 Hf 同位素测试结果见表 2, $\epsilon_{\text{Hf}}(t)$ 值和两阶段模式年龄用岩体谐和年龄计算。24 个分析测试点获得的 $^{176}\text{Yb}/^{177}\text{Hf}$ 、 $^{176}\text{Lu}/^{177}\text{Hf}$ 和 $^{176}\text{Hf}/^{177}\text{Hf}$ 比值分别为 0.009 521~0.081 255、0.000 354~0.002 986 和 0.281 912 0~0.282 486 2。数据可见绝大多数锆石 Hf 同位素测点的 $^{176}\text{Lu}/^{177}\text{Hf}$ 比值都小于 0.002

表 3 祁连山西段硫磺矿北花岗闪长岩的全岩主量元素(%)和微量元素(10^{-6})组成Table 3 Whole-rock major element (%) and trace element (10^{-6}) compositions for granodiorites in northern Liuhuangkuang, Western Qilian

| 样品 | D2864-H1 | D2864-H2 | D2864-H3 | D2864-H4 | D2864-H5 | D2864-H6 | D2864-H7 | D2864-H8 | D2864-H9 | D2864-H10 | D2864-H11 |
|---|----------|----------|----------|----------|----------|----------|----------|----------|----------|-----------|-----------|
| SiO ₂ | 60.55 | 60.57 | 61.41 | 60.71 | 59.47 | 61.25 | 62.13 | 61.23 | 62.11 | 62.96 | 60.77 |
| TiO ₂ | 0.45 | 0.58 | 0.40 | 0.54 | 0.53 | 0.53 | 0.56 | 0.59 | 0.54 | 0.59 | 0.47 |
| Al ₂ O ₃ | 15.81 | 14.52 | 15.74 | 15.12 | 15.59 | 15.53 | 15.13 | 15.29 | 15.31 | 14.56 | 15.42 |
| Fe ₂ O ₃ ^T | 6.69 | 8.92 | 6.30 | 7.68 | 7.32 | 6.59 | 6.91 | 7.96 | 6.16 | 6.97 | 7.34 |
| MnO | 0.12 | 0.16 | 0.12 | 0.16 | 0.14 | 0.18 | 0.15 | 0.11 | 0.15 | 0.18 | 0.14 |
| MgO | 3.24 | 4.11 | 3.11 | 3.53 | 3.64 | 3.20 | 3.26 | 3.22 | 2.99 | 2.68 | 3.28 |
| CaO | 3.21 | 3.28 | 3.70 | 4.18 | 3.04 | 4.37 | 3.01 | 3.58 | 3.46 | 3.51 | 3.96 |
| Na ₂ O | 4.19 | 2.69 | 3.41 | 2.93 | 3.93 | 3.18 | 3.80 | 2.67 | 3.08 | 3.27 | 3.15 |
| K ₂ O | 1.66 | 2.04 | 2.60 | 2.05 | 2.37 | 1.93 | 2.32 | 2.44 | 2.70 | 2.48 | 2.21 |
| P ₂ O ₅ | 0.12 | 0.14 | 0.12 | 0.13 | 0.14 | 0.12 | 0.12 | 0.14 | 0.13 | 0.12 | 0.14 |
| LOI | 3.75 | 2.92 | 3.08 | 2.96 | 3.38 | 2.98 | 2.07 | 2.71 | 2.88 | 2.42 | 3.14 |
| Total | 99.8 | 99.93 | 100 | 99.99 | 99.56 | 99.88 | 99.45 | 99.93 | 99.5 | 99.74 | 100.02 |
| Mg [#] | 53.02 | 51.8 | 53.53 | 51.73 | 53.69 | 53.1 | 52.38 | 48.51 | 53.09 | 47.31 | 51.05 |
| A/CNK | 1.09 | 1.15 | 1.04 | 1.03 | 1.07 | 1.02 | 1.06 | 1.13 | 1.07 | 1.01 | 1.04 |
| FeO ^T | 6.02 | 8.03 | 5.67 | 6.91 | 6.58 | 5.93 | 6.21 | 7.16 | 5.54 | 6.27 | 6.60 |
| Rb | 77.37 | 88.01 | 110.60 | 70.68 | 91.68 | 69.12 | 80.87 | 100.9 | 108.1 | 84.84 | 82.26 |
| Sr | 180.40 | 235.50 | 221.80 | 164.60 | 121.90 | 176.50 | 116.60 | 188.30 | 213.60 | 163.60 | 158.40 |
| Ba | 262.70 | 600.60 | 482.20 | 451.60 | 407.40 | 411.60 | 426.30 | 543.90 | 565.00 | 506.40 | 443.80 |
| Th | 10.32 | 10.22 | 10.29 | 10.07 | 9.92 | 9.40 | 10.38 | 10.67 | 10.62 | 10.43 | 11.30 |
| U | 1.92 | 2.22 | 1.70 | 2.12 | 2.31 | 2.08 | 2.32 | 1.87 | 2.29 | 1.95 | 2.14 |
| Nb | 7.02 | 7.80 | 5.73 | 7.88 | 7.54 | 7.11 | 7.99 | 7.75 | 7.82 | 8.92 | 6.81 |
| Ta | 0.57 | 0.65 | 0.47 | 0.66 | 0.59 | 0.57 | 0.67 | 0.66 | 0.65 | 0.73 | 0.56 |
| Zr | 214.90 | 160.40 | 166.10 | 185.70 | 216.90 | 173.90 | 183.30 | 182.20 | 169.90 | 189.50 | 237.80 |
| Hf | 5.23 | 4.38 | 4.30 | 4.90 | 5.26 | 4.36 | 4.62 | 4.77 | 4.36 | 4.89 | 5.89 |
| Co | 16.69 | 24.16 | 16.22 | 20.01 | 17.39 | 17.53 | 16.97 | 19.52 | 15.45 | 16.16 | 17.69 |
| Ni | 22.19 | 35.03 | 22.76 | 27.17 | 22.71 | 25.33 | 22.74 | 23.63 | 17.82 | 18.84 | 25.27 |
| Cr | 92.55 | 153.6 | 88.68 | 96.12 | 90.07 | 92.31 | 85.14 | 81.47 | 77.79 | 76.3 | 101.2 |
| V | 91.75 | 113.1 | 78.86 | 107 | 90.56 | 97.07 | 89.23 | 106.6 | 84.98 | 96.31 | 90.17 |
| Sc | 14.84 | 19.11 | 13.77 | 16.33 | 15.3 | 14.79 | 15.29 | 16.62 | 14.88 | 15.99 | 15.43 |
| Cs | 3.97 | 2.38 | 3.97 | 1.97 | 6.42 | 2.11 | 2.54 | 2.43 | 3.29 | 2.52 | 3.56 |
| Ga | 19.2 | 18.99 | 19.51 | 19.29 | 20.78 | 19.26 | 19.33 | 18.68 | 19.22 | 19.21 | 19.57 |
| Cu | 11.62 | 14.25 | 14.03 | 18.23 | 15.83 | 16.57 | 10.56 | 15.02 | 12.93 | 7.35 | 15.68 |
| Pb | 47.99 | 25.71 | 14.07 | 30.78 | 12.94 | 30.35 | 17.51 | 9.69 | 15.82 | 9.56 | 17.30 |
| Zn | 111.10 | 123.90 | 78.50 | 140.70 | 78.06 | 154.80 | 119.60 | 74.25 | 117.30 | 107.10 | 109.70 |
| Ti | 2 918 | 3 634 | 2 365 | 3 551 | 3 063 | 3 133 | 3 362 | 3 439 | 3 197 | 3 617 | 3 028 |
| La | 23.15 | 54.01 | 26.08 | 30.40 | 26.96 | 26.71 | 29.70 | 25.07 | 28.23 | 28.55 | 27.63 |
| Ce | 47.81 | 114.5 | 52.04 | 61.55 | 55.51 | 53.25 | 59.84 | 50.79 | 58.37 | 57.75 | 56.14 |
| Pr | 5.72 | 12.86 | 6.20 | 7.19 | 6.51 | 6.41 | 7.04 | 5.95 | 6.71 | 6.69 | 6.7 |
| Nd | 21.84 | 43.64 | 23.04 | 27.09 | 24.56 | 23.88 | 26.35 | 22.53 | 25.57 | 24.73 | 25.28 |
| Sm | 4.81 | 8.02 | 4.9 | 5.67 | 5.21 | 4.92 | 5.53 | 4.86 | 5.29 | 5.27 | 5.42 |
| Eu | 0.86 | 0.79 | 0.95 | 1.05 | 1.03 | 1.04 | 1.03 | 0.93 | 0.97 | 0.94 | 1.05 |
| Gd | 4.38 | 6.81 | 4.47 | 5.15 | 4.81 | 4.52 | 5.01 | 4.45 | 4.87 | 4.79 | 4.97 |
| Tb | 0.65 | 0.89 | 0.64 | 0.72 | 0.70 | 0.64 | 0.72 | 0.66 | 0.69 | 0.69 | 0.73 |
| Dy | 3.88 | 4.93 | 3.76 | 4.10 | 4.10 | 3.63 | 4.19 | 3.88 | 4.00 | 4.07 | 4.22 |
| Ho | 0.78 | 0.94 | 0.76 | 0.82 | 0.82 | 0.72 | 0.83 | 0.78 | 0.79 | 0.82 | 0.83 |
| Er | 2.16 | 2.54 | 2.05 | 2.21 | 2.29 | 1.96 | 2.29 | 2.16 | 2.17 | 2.26 | 2.29 |
| Tm | 0.32 | 0.38 | 0.30 | 0.33 | 0.33 | 0.29 | 0.33 | 0.32 | 0.33 | 0.34 | 0.35 |
| Yb | 2.11 | 2.40 | 1.96 | 2.11 | 2.17 | 1.89 | 2.17 | 2.10 | 2.07 | 2.26 | 2.25 |
| Lu | 0.32 | 0.36 | 0.30 | 0.32 | 0.34 | 0.29 | 0.33 | 0.32 | 0.32 | 0.34 | 0.34 |
| Y | 20.28 | 22.94 | 19.54 | 20.85 | 21.89 | 18.80 | 21.13 | 20.14 | 20.65 | 20.70 | 21.37 |
| K | 13 816 | 16 949 | 21 619 | 16 996 | 19 650 | 16 006 | 19 240 | 20 222 | 22 418 | 20 587 | 18 338 |
| P | 534 | 590 | 513 | 576 | 617 | 542 | 539 | 596 | 564 | 527 | 606 |
| ∑REE | 118.79 | 253.07 | 127.45 | 148.71 | 135.34 | 130.15 | 145.36 | 124.80 | 140.38 | 139.50 | 138.20 |
| LREE | 104.19 | 233.82 | 113.21 | 132.95 | 119.78 | 116.21 | 129.49 | 110.13 | 125.14 | 123.93 | 122.22 |
| HREE | 14.60 | 19.25 | 14.24 | 15.76 | 15.56 | 13.94 | 15.87 | 14.67 | 15.24 | 15.57 | 15.98 |
| LREE/HREE | 7.14 | 12.15 | 7.95 | 8.44 | 7.70 | 8.34 | 8.16 | 7.51 | 8.21 | 7.96 | 7.65 |
| La _N /Yb _N | 7.87 | 16.17 | 9.55 | 10.32 | 8.92 | 10.14 | 9.81 | 8.55 | 9.78 | 9.06 | 8.82 |
| δEu | 0.57 | 0.33 | 0.62 | 0.59 | 0.63 | 0.68 | 0.60 | 0.61 | 0.58 | 0.57 | 0.62 |
| Nb/Ta | 12.32 | 12.00 | 12.19 | 11.94 | 12.78 | 12.47 | 11.93 | 11.74 | 12.03 | 12.22 | 12.16 |
| La/Nb | 3.30 | 6.92 | 4.55 | 3.86 | 3.58 | 3.76 | 3.72 | 3.23 | 3.61 | 3.20 | 4.06 |
| Th/Nb | 1.47 | 1.31 | 1.80 | 1.28 | 1.32 | 1.32 | 1.30 | 1.38 | 1.36 | 1.17 | 1.66 |
| Th/La | 0.45 | 0.19 | 0.39 | 0.33 | 0.37 | 0.35 | 0.35 | 0.43 | 0.38 | 0.37 | 0.41 |
| Rb/Sr | 0.43 | 0.37 | 0.50 | 0.43 | 0.75 | 0.39 | 0.69 | 0.54 | 0.51 | 0.52 | 0.52 |
| Rb/Nb | 11.02 | 11.28 | 19.30 | 8.97 | 12.16 | 9.72 | 10.12 | 13.02 | 13.82 | 9.51 | 12.08 |

注: Fe₂O₃^T 为全铁, A/CNK = Al₂O₃ / (CaO + Na₂O + K₂O), 式中氧化物全为摩尔数; Mg[#] = 100 × MgO / (MgO + Fe₂O₃^T), 式中氧化物全为摩尔数; La_N / Yb_N 为球粒陨石标准化值, δEu = Eu_N / (Sm_N + Gd_N)^{1/2}.

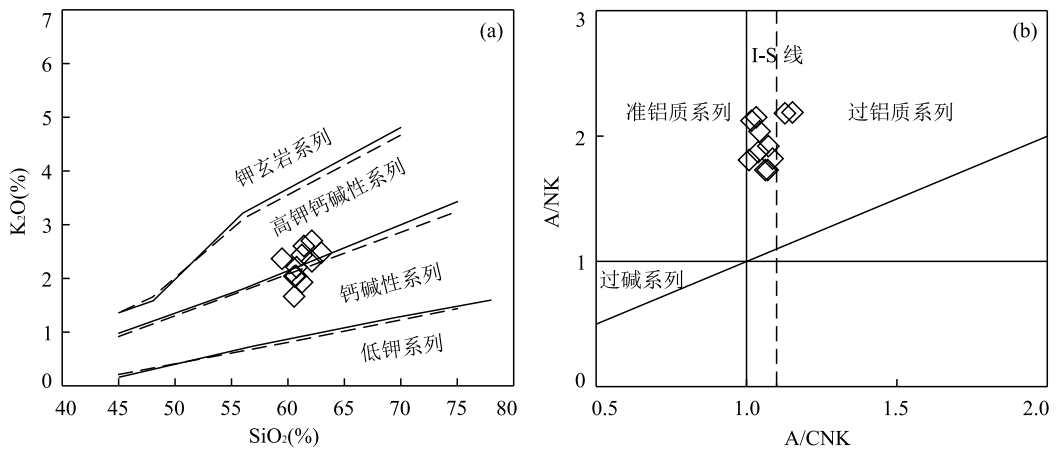


图 4 硫磺矿北花岗闪长岩 K_2O vs. Si_2O 图解(a)和 A/NK vs. A/CNK 图解(b)

Fig.4 Diagrams of K_2O vs. Si_2O and A/NK vs. A/CNK for granodiorites in northern Liuhuangkuang, Western Qilian

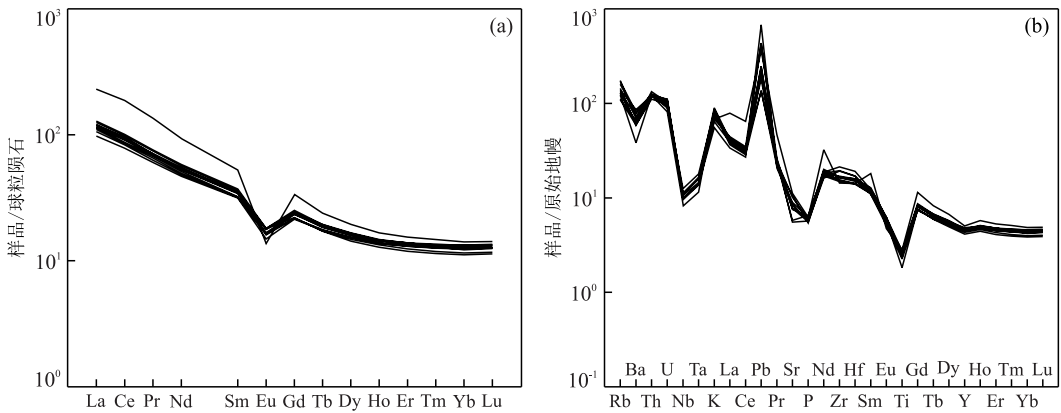


图 5 硫磺矿北花岗闪长岩稀土元素球粒陨石标准化分布形式图解(a)和微量元素原始地幔标准化多元素图解(b)

Fig.5 Chondrite-normalized REE patterns (a) and primitive mantle-normalized multi-element diagram (b) for granodiorites in northern Liuhuangkuang, Western Qilian

球粒陨石标准数据采用 McDonough and Sun(1995)

Ti)、Sr 和 P 的特征,与火山弧花岗岩的特征相似(图 5b, 杜德道等, 2011)。在图 5 上,除了样品 D2864-H2 稍有区别外,其余样品具有一致的分布形式。样品中反映岩石演化特征的元素比值 $Nb/Ta=11.74\sim 12.78$, $La/Nb=3.20\sim 6.92$, $Th/Nb=1.17\sim 1.80$, $Th/La=0.19\sim 0.45$, $Rb/Sr=0.37\sim 0.75$, $Rb/Nb=8.97\sim 19.30$ 。

4 讨论

4.1 岩石成因

张旗等(1997, 2006, 2008)认为花岗岩最重要的是源区特征,其次是部分熔融程度、温度、压力及挥发成分的加入情况。研究表明:在准铝质和弱过铝质岩浆中,磷灰石溶解度很低,在岩浆分异过程中随 SiO_2

含量增加而降低;相反,磷灰石在强过铝质岩浆中未达到饱和,其溶解度相对较高,因此, P_2O_5 含量随 SiO_2 含量增加而呈现基本不变或者增加的趋势(Wolf and London, 1994),而且这个特征已广泛的用于判别 I 型和 S 型花岗岩(Wolf and London, 1994)。硫磺矿北岩体的 P_2O_5 (小于 0.14%) 含量较低,并随 SiO_2 含量增加而减少,显示出 I 型花岗岩的演化趋势(图 6a)。在 Na_2O vs. K_2O 图解上(图 6b),所有样品仍然落入 I 型花岗岩区域。本文样品的 A/CNK 为 1.01~1.15,具有 I 型花岗岩的特征。Y 和 Rb 或者 Th 和 Rb 的线性关系也可以用于鉴别 I/S 型花岗岩,通常情况下, I 型花岗岩的 Y 和 Th 含量与 Rb 含量呈正相关,而在 S 型花岗岩中 Y 和 Th 含量随 Rb 含量增加而减少(Chappell and White, 2001)。本文样品的 Y 和 Th 含量随 Rb 含量增加而呈现基本不变的趋势(图 6c、6d),具 I 型花岗岩的特征。前述分析表明硫磺矿北岩

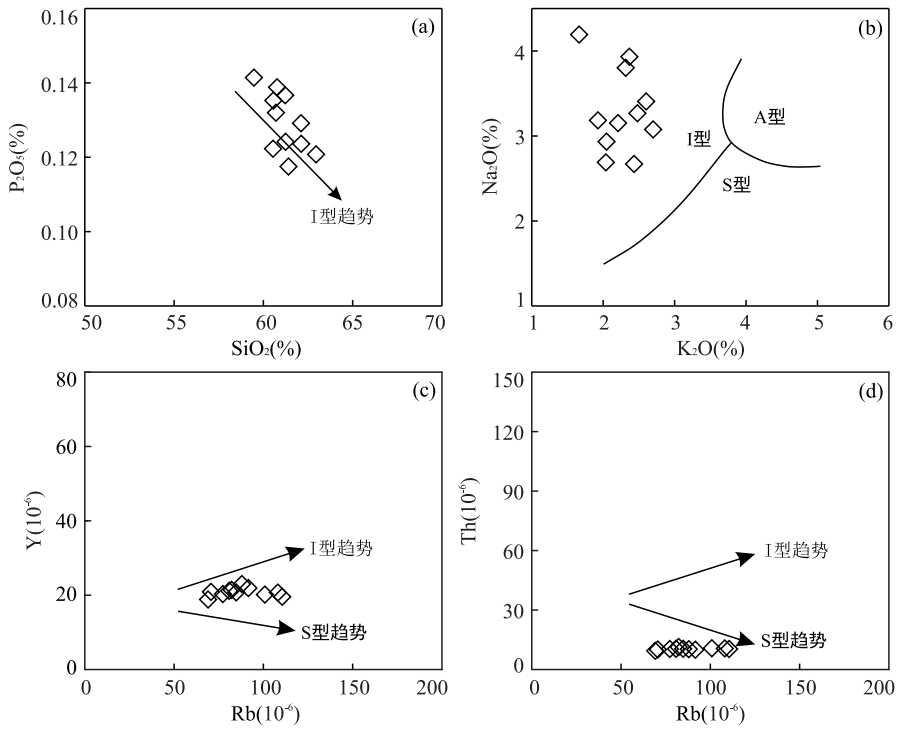


图 6 花岗岩类型判别图解

Fig.6 Discrimination diagrams of granite type

据 Zorpi *et al.*(1989)

体为 I 型花岗岩。

硫磺矿北花岗闪长岩具有一定程度高硅 (59.47%~62.96%)、相对中等质量分数的 Al₂O₃ (14.52%~15.81)、MgO 及弱过铝质到过铝质等主量元素特征,岩石具有大离子亲石元素和不相容元素如 Rb、Th 和 U 等富集,明显亏损高场强元素 (Nb、Ta、Ti) 及 Sr、P 的特征,反映了地壳源区特点 (Mckenzie, 1989). 前人研究表明: Ta、Nb 和 Ti 亏损暗示岩浆可能与地壳混染作用 (Mckenzie, 1989) 或者源区经历了俯冲过程中流体交代作用有关 (Sun and McDonough, 1989), 而不可能是由软流圈部分熔融直接产生 (Foley, 1992). 研究表明: Nb 和 Ta 两种元素化学性质相似, 因此, Nb/Ta 比值在岩浆分异中不会造成较大的分异, 可以指示岩浆源区特征及演化过程 (Green, 1995). 通常幔源岩浆的 Nb/Ta 比值为 17.5±2, 壳源岩浆的 Nb/Ta 比值为 11~12 (Green, 1995), 研究区 11 件花岗闪长岩样品 Nb/Ta 比值为 11.74~12.78, 可以反映出岩浆的壳源特点; La/Nb 值在 3.23~6.92 之间, 均大于 1, 表明岩石源于壳源 (Depaolo and Daley, 2000). 前人研究表明 MORB 和 OIB 中 Nb/U 比值较高 (47±10), 原始地幔中 Nb/U 平均比值为 33.59, 但大陆地壳中该比值通常很低 (Taylor and McLennan, 1985), 研

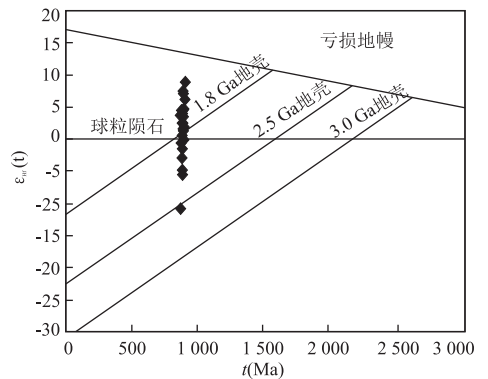


图 7 样品 $\epsilon_{\text{Hf}}(t)-t$ 图解

Fig.7 $\epsilon_{\text{Hf}}(t)$ versus t diagram of the granodiorite

究区花岗闪长岩低的 Nb/U 值 (3.26~4.57) (表 4) 远低于前两者比值; 另外, 研究区样品 Sm/Nd 比值在 0.18~0.22 之间, 与大陆地壳的 Sm/Nd 比值 (0.17~0.25) 相近, 反映岩石组分多源于地壳 (张延军等, 2016; 陈加杰等, 2016); 综上所述, 硫磺矿北花岗闪长岩的微量元素显示出壳源特点。

硫磺矿北花岗闪长岩体的 $\epsilon_{\text{Hf}}(t)$ 值在 -10.8~8.9 之间, 主要位于 0~7 之间, 多表现为正值, 二阶段地壳模式年龄主要在 1 247~1 801 Ma 之间. 在 $t-\epsilon_{\text{Hf}}(t)$ 图解中 (图 7), 样品均落在球粒陨石演化线附近, 大多数位于该线之上, 表明成岩过程中主要为

表 4 祁连山新元古代岩浆事件年龄统计

Table 4 Zircon U-Pb ages of Neoproterozoic magmatic events in Qilian Mountains

| 地质体 | 年龄(Ma) | 测试方法 | 资料来源 |
|-------------|---------------|-----------|---------------------------|
| 中祁连响河花岗岩 | 917±12 | TIMS | 郭进京等(2000) |
| 中祁连湟源群变质火山岩 | 910.0±6.7 | TIMS | 郭进京等(2000) |
| 中祁连黑云母二长花岗岩 | 943±28 | TIMS | 万渝生等(2003) |
| 祁连地块片麻状花岗岩 | 930±8, 918±14 | SHRIMP | 董国安等(2007) |
| 祁连地块东段五峰村岩体 | 846±2 | | |
| 祁连地块东段五间房岩体 | 853±2 | LA-ICP-MS | Yong <i>et al.</i> (2008) |
| 祁连地块东段向河岩体 | 888±3 | | |
| 中祁连化隆群 | 770~950 | SHRIMP | Yang <i>et al.</i> (2015) |
| 祁连东段片麻状花岗岩 | 880~900 | LA-ICP-MS | 徐旺春等(2007) |
| 中祁连片麻状花岗岩 | 875±8 | LA-ICP-MS | 徐学义等(2008) |
| 中祁连黑云斜长片麻岩 | 910±7 | LA-ICP-MS | 余吉远等(2012) |

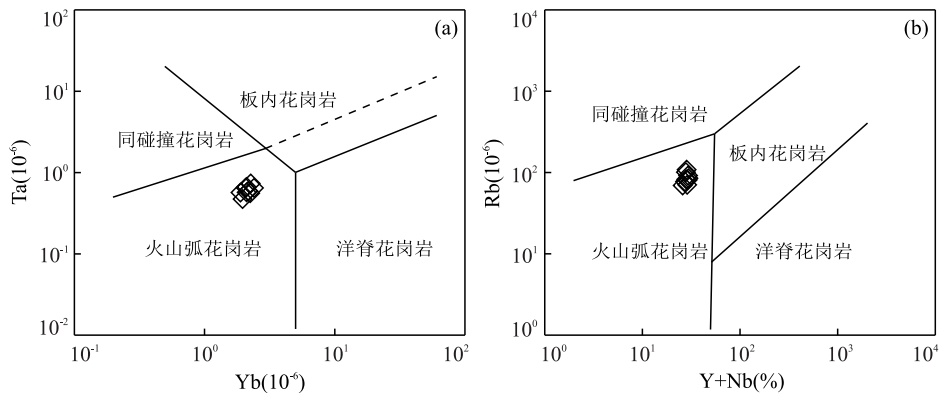


图 8 Yb-Ta、Y+Nb-Rb 构造环境图解

Fig.8 Yb-Ta and Y+Nb-Rb discrimination diagrams for the tectonic interpretation of granites

年轻组分的加入,也有古老地壳物质重熔的组分.年轻组分参与花岗岩成岩过程的方式可能有两种情况,其一为幔源岩浆与其诱发的地壳物质部分熔融形成的长英质岩浆在地壳深部混合形成壳幔混源岩浆;另一种是幔源岩浆首先侵入到地壳基底岩石中形成初生地壳,然后在后期热事件的影响下,这种既有初生地壳又有古老基底地壳构成的混合地壳原岩发生部分熔融(吴福元等,2007).Vervoot 等认为具有正 $\epsilon_{\text{Hf}}(t)$ 值的花岗质岩石来自亏损地幔或从亏损地幔中新生的年轻地壳物质的部分熔融,负 $\epsilon_{\text{Hf}}(t)$ 值则表明地壳 Hf 同位素为主导(Vervoot *et al.*, 2000; Griffin and Belousova, 2004).样品具有高 $\epsilon_{\text{Hf}}(t)$ 锆石,表明亏损地幔中新生的年轻地壳物质的部分熔融参与到花岗闪长岩的形成.结合本次研究认为,研究区花岗闪长岩的岩浆源区初始物质主要来源于中元古代增生的年轻地壳熔融,并经历一定程度地分离结晶,可能也有古老地壳物质的参与.

4.2 构造背景及地质意义

前人研究表明,新元古代时期岩浆活动在祁连

地块较为活跃(表 4):郭进京等(1999, 2000)分别在中祁连湟源群中获取响河花岗岩锆石 U-Pb TIMS 年龄时代为 917 ± 12 Ma,变质火山岩 U-Pb TIMS 年龄为 910.0 ± 6.7 Ma;万渝生等(2003)在中祁连黑云母二长花岗岩中获取锆石 U-Pb TIMS 年龄为 943 ± 28 Ma,同时在黑云母斜长片麻岩中获取 940 ± 30 Ma 年龄数据;董国安等(2007)在湟源群中的片麻状花岗岩获取锆石 SHRIMP 年龄为 930 ± 8 Ma,在马衔山群片麻状花岗岩中获取锆石 U-Pb SHIMP 年龄为 918 ± 14 Ma;徐旺春等(2007)在祁连地块东段化隆群片麻状花岗岩中获取锆石 U-Pb 年龄集中于 $880 \sim 900$ Ma,同时,徐学义等(2007)在化隆群中获取片麻状花岗岩形成时代为 875 ± 8 Ma,二者年龄保持一致;另外,雍拥等(2008)在祁连地块东段五峰村岩体、五间房岩体、向河岩体分别获取锆石 U-Pb LA-ICP-MS 年龄为 846 ± 2 Ma、 853 ± 2 Ma 和 888 ± 3 Ma;余吉远等(2012)在化隆群黑云斜长片麻岩中获取碎屑锆石年龄主峰值 910 ± 7 Ma;Yang *et al.*(2015)在化隆群研究中获取

大量花岗质片麻岩锆石 U-Pb SHRIMP 年龄分布在 770~950 Ma 之间。前述学者获得大量新元古代早期岩浆活动年代学资料,而本文硫磺矿北岩体的锆石 U-Pb 年龄(926±4 Ma),与上述岩体岩浆活动时保持一致,形成于新元古代早期。硫磺矿北岩体具有富集 Th 和 U,亏损 Nb、Ta 和 Ti 的特征,这种特征通常出现在火山弧环境的岩石中(Collins *et al.*, 2008;陶刚等,2016),同时 La/Nb 平均值为 3.98,这也与 Salters and Hart 认为的活动大陆边缘区 La/Nb 值(大于 2)是相符的(Salters and Hart, 1991)。在 Yb-Ta 和 Y+Nb-Rb 构造图解中(Pearce *et al.*, 1984, 1996),样品全部落入火山弧构造环境中。另外,郭进京等(1999)对湟源群中变质杂砂岩和变质中基性火山岩研究认为湟源群的沉积大地构造背景应为活动大陆边缘,其中变质基性火山岩地球化学特征显示出类似于岛弧火山岩特征;万渝生等(2003)认为通过研究祁连前寒武纪深变质基底中壳源花岗质岩石认为祁连地块新元古代岩浆形成于活动大陆边缘环境,并总结出祁连地块前寒武系基底模式年龄在 1 870~2 260 Ma 之间,而硫磺矿北花岗闪长岩岩体构造环境显示其形成于活动大陆边缘, Hf 同位素 T_{DM2} 模式年龄显示为 1 247~2 451 Ma,与前人研究具有高度一致性。因此,可以推断中祁连在新元古代可能为活动大陆边缘环境,而硫磺矿北花岗闪长岩为中元古代增生的年轻地壳部分熔融的产物,并经历一定程度地分离结晶,可能也有古老地壳部分熔融成分参与该岩体形成。

值得关注的是祁连地块亲缘性目前有两种观点:传统观点认为祁连地块为华北板块不同程度裂解“开—合构造”演化,即北祁连和中祁连发生大陆裂解后,裂隙逐渐向南迁移,进而引起南祁连与中祁连的分离,进一步发育成洋盆,而后又与中祁连发生俯冲—碰撞完成拼合(左国朝等,1987;冯益民等,1996);另一种新的观点认为祁连地块与扬子地块有较强的亲缘性,在新元古代时应同属于冈瓦纳大陆一部分(万渝生等,2003;董国安等,2007;徐旺春等,2007;Tung *et al.*, 2013)。近年来,不同学者对祁连地块前寒武纪基底岩石碎屑锆石 U-Pb 年龄数据显示祁连地块大量分布元古代年龄信息(万渝生等,2003;董国安等,2007;Tung *et al.*, 2013),研究区青白口系沉积岩碎屑锆石中也存在新古代年龄峰值(项目内部数据,待发表),而华北克拉通却不存在该阶段年龄信息(第五春荣等,2012)。目前较为合理的解释就是新元古代对罗迪尼亚超大陆(Rodinia)汇

聚事件在祁连地块存在响应,与华北克拉通迥异,在新元古代时祁连地块可能同属于冈瓦纳大陆一部分。本文硫磺矿北岩体形成时代为 926±4 Ma,为新元古代早期,并具有陆缘弧性质,很可能为祁连地块在中元古代时期对全球 Rodinia 超大陆聚合事件响应的岩浆产物,为祁连地块属性提供可信的新元古代岩浆活动证据。

5 结论

(1)本文获得硫磺矿岩体中锆石岩浆振荡环带的 LA-ICP-MS U-Pb 年龄为 926±4 Ma,属于新元古代岩浆活动产物,与祁连地块大量中新元古代岩浆活动时间一致。

(2)硫磺矿北岩体岩性为花岗闪长岩,其 SiO₂ 含量在 59.47%~62.96% 之间,平均为 61.19%, Na₂O/K₂O>1.0, 铝饱和指数 A/CNK 为 1.01~1.15,为一套属弱过铝质的高钾钙碱性 I 型花岗岩。微量和稀土元素组成上具有富集大离子亲石元素和不相容元素(Rb、Th 和 U),亏损高场强元素 Nb、Ta、Ti、Sr 和 P,明显富集轻稀土,具有中等—强 Eu 负异常。

(3)锆石 Hf 同位素分析结果显示, $\epsilon_{\text{Hf}}(t)$ 主要位于 0~7 之间,二阶段地壳模式年龄 T_{DM2} 为 1 247~2 451 Ma,与祁连地区产出的新元古代花岗岩具有一致性,结合全岩地球化学推断中祁连在新元古代可能为活动大陆边缘环境,而硫磺矿北花岗闪长岩为中元古代增生的年轻地壳部分熔融的产物,经历一定程度分离结晶,可能也有古老地壳部分熔融成分参与该岩体形成。该时期岩浆活动可能属于对新元古代 Rodinia 超大陆汇聚事件的响应,为祁连地块属性提供可信研究资料。

References

- Altherr, R., Holl, A., Hegner, E., et al., 2000. High-Potassium, Calc-Alkaline I-Type Plutonism in the European Variscides: Northern Vosges (France) and Northern Schwarzwald (Germany). *Lithos*, 50: 51–73. doi: 10.1016/S0024-4937(99)00052-3
- Andersen, T., Griffin, W. L., Sylvester, A. G., 2007. Sveconorwegian Crustal Underplating in Southwestern Fennoscandia: LAM-ICPMS U-Pb and Lu-Hf Isotope Evidence from Granites and Gneisses in Telemark, Southern Norway. *Lithos*, 93(3–4): 273–287. doi: 10.1016/j.lithos.2006.03.068

- Blichert-Toft, J., Chauvel, C., Albarède, F., 1997. Separation of Hf and Lu for High-Precision Isotope Analysis of Rock Samples by Magnetic Sector-Multiple Collector ICP-MS. *Contributions to Mineralogy & Petrology*, 127(3): 248—260. doi: 10.1007/s004100050278
- Bureau of Geology and Mineral Resources of Qinghai, 1991. Regional Geology of Qinghai Province, Geological Publishing Press, Beijing (in Chinese).
- Chappell, B. W., White, A. J. R., 2001. Two Contrasting Granite Types; 25 Years Later. *Australian Journal of Earth Sciences*, 48(4): 489—499. doi: 10.1046/j.1440-0952.2001.00882.x
- Chen, J. F., Foland, K. A., Xing, F. M., et al., 1991. Magmatism along the Southeast Margin of the Yangtze Block; Precambrian Collision of the Yangtze and Cathaysia Blocks of China. *Geology*, 19(8): 815. doi: 10.1130/0091-7613(1991)019<0815:matsmo>2.3.co;2
- Chen, J. J., Fu L. B., Wei J. H., et al., 2009. Geochemical Characteristics of Late Ordovician Granodiorite in Gouli Area, Eastern Kunlun Orogenic Belt, Qinghai Province; Implications on the evolution of Proto-Tethys Ocean. *Earth Science*, 41(11): 1863—1882 (in Chinese with English abstract).
- Collins, W. J., Richards, S. W., 2008. Geodynamic Significance of S-Type Granites in Circum-Pacific Orogens. *Geology*, 36(7): 559. doi: 10.1130/g24658a.1
- Depaolo, D. J., Daley, E. E., 2000. Neodymium Isotopes in Basalts of the Southwest Basin and Range and Lithospheric Thinning during Continental Extension. *Chemical Geology*, 169(1): 157—185.
- Diwu, C. R., Sun, Y., Wang, Q., 2012. The Crustal Growth and Evolution of North China Craton; Revealed by Hf Isotopes in Detrital Zircons from Modern Rivers. *Acta Petrologica Sinica*, 28(11): 3520—3530 (in Chinese with English abstract).
- Dong, G. A., Yang, H. R., Yang, H. Y., et al., 2007. the Zircon SHIMP U-Pb Dating and Its Significance of the Precambrian Basement, Qilian Terrance. *Chinese Science Bulletin*, 52(13): 1572—1585 (in Chinese with English abstract).
- Du, D. D., Qu, X. M., Wang, G. H., et al., 2011. Bidirectional Subduction of the Middle Tethys Oceanic Basin in the West Segment of Bangonghu-Nujiang Suture, Tibet: Evidence from Zircon U-Pb LAICPMS Dating and Petrogeochemistry of Arc Granites. *Acta Petrologica Sinica*, 27(7): 1993—2002 (in Chinese with English abstract).
- Du, Y. S., Zhu, J., Gu, S. Z., 2006. Sedimentary Geochemistry and Tectonic Significance of ordovician Cherts in Sunan, North Qilian Mountains. *Earth Science*, 31(1): 101—109 (in Chinese).
- Du, D. D., Qu, X. M., Wang, G. H., et al., 2011. Bidirectional Subduction of the Middle Tethys Oceanic Basin in the West Segment of Bangonghu-Nujiang Suture, Tibet: Evidence from Zircon U-b LAICPMS Dating and Petrogeochemistry of Arc Granites. *Acta Petrologica Sinica*, 27(7): 1993—2002 (in Chinese with English Abstract).
- Feng, Y. M., He, S. P., 1996. The Tectonic and Orogenic Process of Qilian Mountains. Geological Press, Beijing (in Chinese without English Abstract).
- Feng, Y. M., 1997. Investigatory Summary of the Qilian Orogenic Belt, China: History, Presence and Prospect. *Advence in Earth Sciences*, 12(4): 5—12 (in Chinese with English abstract).
- Feng, Y. M., He, S. P., 1995. Research for Geology and Geochemistry of Several ophiolites in the North Qilian Mountains, China. *Acta Petrologica Sinica*, 11(S1): 125—140, 142—146 (in Chinese with English abstract).
- Foley, S., 1992. Vein-Plus-Wall-Rock Melting Mechanisms in the Lithosphere and the Origin of Potassic Alkaline Magmas. *Lithos*, 28(3—6): 435—453. doi: 10.1016/0024-4937(92)90018-t
- Gehrels, G. E., Yin, A., Wang, X. F., 2003. Magmatic History of the Northeastern Tibetan Plateau. *Journal of Geophysical Research: Solid Earth*, 108(B9): 1—10. doi: 10.1029/2002jb001876
- Green, T. H., 1995. Significance of Nb/Ta as an Indicator of Geochemical Processes in the Crust-Mantle System. *Chemical Geology*, 120(3—4): 347—359. doi: 10.1016/0009-2541(94)00145-x
- Greentree, M. R., Li, Z. X., Li, X. H., et al., 2006. Late Mesoproterozoic to Earliest Neoproterozoic Basin Record of the Sibao Orogenesis in Western South China and Relationship to the Assembly of Rodinia. *Precambrian Research*, 151(1—2): 79—100. doi: 10.1016/j.precamres.2006.08.002
- Griffin, W. L., Wang, X., Jackson, S. E., et al., 2002. Zircon Chemistry and Magma Mixing, SE China: In-Situ Analysis of Hf Isotopes, Tonglu and Pingtan Igneous Complexes. *Lithos*, 61(3—4): 237—269. doi: 10.1016/s0024-4937(02)00082-8
- Guan, J. L., Geng, Q. R., Peng, Z. M., et al., 2016. Petrology, Petrochemistry and Zircon U-Pb Dating and Hf Isotope Features of Xiamari Granites in Tanggula Magmatic Belt, Qinghai-Tibet Plateau. *Acta Geologica Sinica*, 90(2): 304—333 (in Chinese with English Abstract).
- Guo, J. J., Zhao, F. Q., Li, H. K., et al., 2000. New Chronologi-

- cal Evidence of the Age of Huangyuan Group in the Eastern Segment of Mid-Qilian Massif and its Geological Significance. *Regional Geology of China*, 19(1): 26—31 (in Chinese with English abstract).
- Guo, Y.S., Sun, S.R., Fu, X.M., 1993. Characteristics of Trace Elements for the Ultrabasic Rocks of Ophiolite in the Western Part of the North Qilian and its Geological Significance. *Journal of Lanzhou University: Natural Science Edition*, (3): 206—212 (in Chinese with English abstract).
- Guo, J.J., Zhang, G.W., Lu, S.N., et al., 1999. A discussion on the Proterozoic Stratigraphy Framework in the Basement of Eastern Section of the Mid-Qilian Massif. *Regional Geology of China*, 14(4): 379—382 (in Chinese with English Abstract).
- He, J.W., Zhu, W.B., Ge, R.F., et al., 2014. Detrital Zircon U-Pb Ages and Hf Isotopes of Neoproterozoic Strata in the Aksu Area, Northwestern Tarim Craton: Implications for Supercontinent Reconstruction and Crustal Evolution. *Precambrian Research*, 254: 194—209. doi: 10.1016/j.precamres.2014.08.016
- Hou, K.J., Li, Y.H., Tian, Y.R., 2009. In Situ U-Pb Zircon Dating Using Laser Ablation-Multi Ion Counting-ICP-MS. *Mineral Deposits*, 28(4): 481—492 (in Chinese with English abstract).
- Huang, Z.B., Zheng, J.P., Li, B.H., et al., 2016. Age and Geochemistry of the Early Paleozoic Back-arc Type Ophiolite in Dadaoerji Area, South Qilian, China. *Geotectonica et Metallogenia*, 40(4): 826—838 (in Chinese with English Abstract).
- Jiang, G.L., Zhang, S., Liu, K.F., et al., 2014. Evolution of Neoproterozoic-Mesozoic Sedimentary Basins in Qilian-Qaidam-East Kunlun Are. *Earth Science*, 39(8): 1000—1016 (in Chinese with English Abstract).
- Kemp, A.I.S., Hawkesworth, C.J., Foster, G.L., et al., 2007. Magmatic and Crustal Differentiation History of Granitic Rocks from Hf-O Isotopes in Zircon. *Science*, 315(5814): 980—983. doi: 10.1126/science.1136154
- Knudsen, T. L., Griffin, W., Hartz, E., et al., 2001. In-Situ Hafnium and Lead Isotope Analyses of Detrital Zircons from the Devonian Sedimentary Basin of NE Greenland: A Record of Repeated Crustal Reworking. *Contributions to Mineralogy and Petrology*, 141(1): 83—94. doi: 10.1007/s004100000220
- Li, J.F., Zhang, Z.C., Han, B.F., 2010. Geochronology and Geochemistry of Early Paleozoic Granitic Plutons from Sabei and Shibaocheng Areas, the Western Segment of Central Qilian and their Geological Implications. *Acta Petrologica Sinica*, 26(8): 2431—2444 (in Chinese with English abstract).
- Li, X.H., Li, W.X., Li, Z.X., 2007. On the Genetic Classification and Tectonic Implications of the Early Yanshanian Granitoids in the Nanling Range, South China. *Chinese Science Bulletin*, 52(14): 1873—1885. doi: 10.1007/s11434-007-0259-0
- Li, Z.X., Evans, D. A. D., Halverson, G. P., 2013. Neoproterozoic Glaciations in a Revised Global Palaeogeography from the Breakup of Rodinia to the Assembly of Gondwanaland. *Sedimentary Geology*, 294: 219—232. doi: 10.1016/j.sedgeo.2013.05.016
- Li, C. N., 1992. Trace Elements in Igneous Petrology. China University of Geosciences Publishing House, Wuhan (in Chinese).
- Li, Z., Chen, Y.L., Liu, C.Z., et al., 2016. Formation and Evolution History on the Northern Qilian Orogen; the Evidences from Compositions of Rivers' Sediments and Their Zircon U-Pb Ages, Hf Isotopic Compositions. *Acta Geologica Sinica*, 90(2): 267—283 (in Chinese).
- Liu, J.H., Liu, F.L., Ding, Z.J., et al., 2013. U-Pb Dating and Hf Isotope Study of Detrital Zircons from the Zhifu Group, Jiaobei Terrane, North China Craton: Provenance and Implications for Precambrian Crustal Growth and Recycling. *Precambrian Research*, 235: 230—250. doi: 10.1016/j.precamres.2013.06.014
- Liu, Y.S., Hu, Z.C., Zong, K.Q., et al., 2010. Reappraisal and Refinement of Zircon U-Pb Isotope and Trace Element Analyses by LA-ICP-MS. *Chinese Science Bulletin*, 55(15): 1535—1546. doi: 10.1007/s11434-010-3052-4
- Liu, Y., Liu, H.C., Li, X.H., 1996. Simultaneous and Precise Determination of 40 Trace Elements in Rock Samples Using ICP-MS. *Geochimica*, 25(6): 552—558.
- Lu, S.N., Li, H.K., Zhang, C.L., et al., 2008. Geological and Geochronological Evidence for the Precambrian Evolution of the Tarim Craton and Surrounding Continental Fragments. *Precambrian Research*, 160(1—2): 94—107. doi: 10.1016/j.precamres.2007.04.025
- McDonough, W.F., Sun, S.S., 1995. The Composition of the Earth. *Chemical Geology*, 120(3—4): 223—253. doi: 10.1016/0009-2541(94)00140-4
- McKenzie, D., 1989. Some Remarks on the Movement of Small Melt Fractions in the Mantle. *Earth and Planetary Science Letters*, 95(1—2): 53—72. doi: 10.1016/0012-821x(89)90167-2
- Pearce, J.A., Harris, N.B.W., Tindle, A.G., 1984. Trace Element Discrimination Diagrams for the Tectonic Interpretation of Granitic Rocks. *Journal of Petrology*, 25

- (4):956–983.doi:10.1093/petrology/25.4.956
- Pearce, J. A., 1996. Sources and Setting of Granitic Rocks. *Episodes*, 19(4):120–125.
- Pei, X. Z., Li, Z. C., Li, R. B., et al., 2012. LA-ICP-MS U-Pb Ages of Detrital Zircons from the Meta-Detrital Rocks of the Early Palaeozoic Huluhe Group in Eastern Part of Qilian Orogenic Belt: Constraints of Material Source and Sedimentary Age. *Earth Science Frontiers*, 19(5):205–224 (in Chinese with English abstract).
- Qian, Q., Sun, X. M., Zhang, Q., et al., 1999. Lithogeochemical Characteristics of Jiugequan Ophiolite and its Overlying Rock Suites, North Qilian: The Geodynamic Significance. *Geological Review*, 45(S1):1038–1046 (in Chinese with English abstract).
- Qian, J. Q., Gong, B. J., Dou, S. R., et al., 1986. The Proterozoic Stromatolites from the Western Region of the Middle Qilian Mountain. *Gansu Geology*:5:1–32 (in Chinese with English Abstract).
- Qin, H. P., Wu, C. L., Wang, C. S., et al., 2014. LA-ICP-MS Zircon U-Pb Dating and Geochemical Characteristics of High Sr/Y-type Granite from Xigela, Eastern Qilian Area. *Acta Geologica Sinica*, 30(12):3759–3771 (in Chinese with English Abstract).
- Qin, H. P., Wu, C. L., Wang, C. S., et al., 2014. LA-ICP-MS Zircon U-Pb Geochronology and Geochemical Characteristics of Xiagucheng Granite in North Qilian. *Acta Geologica Sinica*, 88(10):1832–1842 (in Chinese with English Abstract).
- Qiu, J. S., Xiao, E., Hu, J., et al., 2008. Petrogenesis of Highly Fractionated I-Type Granites in the Coastal Area of Northeastern Fujian Province: Constraints from Zircon U-Pb Geochronology, Geochemistry and Nd-Hf Isotopes. *Acta Petrologica Sinica*, 24(11):2468–2484 (in Chinese with English abstract).
- Rudnick, R. L., Gao, S., 2003. Composition of the Continental Crust. *Treatise on Geochemistry*, 1–64. doi:10.1016/b0-08-043751-6/03016-4
- Salters, V. J., Hart, S. R., 1991. The Mantle Sources of Ocean Ridges, Islands and Arcs; the Hf-isotope Connection. *Earth & Planetary Science Letters*, 104(2–4):364–380.
- Shu, L. S., Deng, X. L., Zhu, W. B., et al., 2011. Precambrian Tectonic Evolution of the Tarim Block, NW China: New Geochronological Insights from the Quruqtagh Domain. *Journal of Asian Earth Sciences*, 42(5):774–790. doi:10.1016/j.jseae.2010.08.018
- Simon, L. H., Nigel, M. K., 2007. Zircon: Tiny but Timely. *Elements*, 3(1):13–18.
- Söderlund, U., Patchett, P. J., Vervoort, J. D., et al., 2004. The ¹⁷⁶Lu Decay Constant Determined by Lu-Hf and U-Pb Isotope Systematics of Precambrian Mafic Intrusions. *Earth and Planetary Science Letters*, 219(3–4):311–324. doi:10.1016/s0012-821x(04)00012-3
- Song, S. G., Su, L., Li, X. H., et al., 2012. Grenville-Age Orogenesis in the Qaidam-Qilian Block: The Link between South China and Tarim. *Precambrian Research*, 220–221:9–22. doi:10.1016/j.precamres.2012.07.007
- Song, S. G., Niu, Y. L., Su, L., et al., 2013. Tectonics of the North Qilian Orogen, NW China. *Gondwana Research*, 23:1378–1401.
- Song, S. G., Zhang, G. B., Zhang, C., et al., 2013. Dynamic Process of Oceanic Subduction and Continental Collision: Petrological Constraints of HP-UHP Belts in Qilian-Qaidam, the Northern Tibetan Plateau. *Chin Sci Bull*, 58(23):2240–2245 (in Chinese).
- Sun, S. S., McDonough, W. F., 1989. Chemical and Isotopic Systematics of Oceanic Basalts: Implications for Mantle Composition and Processes. *Geological Society, London, Special Publications*, 42(1):313–345. doi:10.1144/gsl.sp.1989.042.01.19
- Taylor, S. R., McLennan, S. M., 1985. The Continental Crust: Its Composition and Evolution, An Examination of the Geochemical Record Preserved in Sedimentary Rocks. *Journal of Geology*, 94(4):632–633.
- Tung, K. A., Yang, H. Y., Liu, D. Y., et al., 2013. The Neoproterozoic Granitoids from the Qilian Block, NW China: Evidence for a Link between the Qilian and South China Blocks. *Precambrian Research*, 235:163–189. doi:10.1016/j.precamres.2013.06.016
- Tung, K. A., Yang, H. Y., Yang, H. J., et al., 2016. Magma Sources and Petrogenesis of the Early-middle Paleozoic Backarc Granitoids from the Central Part of the Qilian Block, NW China. *Gondwana Research*, 38:197–219. doi:10.1016/j.gr.2015.11.012
- Wan, Y. S., Xu, Z. Q., Yang, J. S., et al., 2003. The Precambrian High-Grade Basement of the Qilian Terrane and Neighboring Areas: Its Ages and Compositions. *Acta Geoscientia Sinica*, 24(4):319–324 (in Chinese with English abstract).
- Wang, C., Li, R. S., Smithies, R. H., et al., 2017. Early Paleozoic Felsic Magmatic Evolution of the Western Central Qilian Belt, Northwestern China, and Constraints on Convergent Margin Processes. *Gondwana Research*, 41:301–324. doi:10.1016/j.gr.2015.12.009
- Wang, H. L., He, S. P., Chen, J. L., et al., 2007. LA-ICPMS Dating of Zircon U-Pb and its Tectonic Significance of Maxianshan Granitoid Intrusive Complex, Gansu Prov-

- ince. *Acta Geologica Sinica*, 81(1): 72—78 (in Chinese with English abstract).
- Wen, B., Evans, D. A. D., Li, Y. X., 2017. Neoproterozoic Paleogeography of the Tarim Block: An Extended or Alternative “Missing-Link” Model for Rodinia? *Earth and Planetary Science Letters*, 458: 92—106. doi: 10.1016/j.epsl.2016.10.030
- Wolf, M. B., London, D., 1994. Apatite Dissolution into Peraluminous Haplogranitic Melts: An Experimental Study of Solubilities and Mechanisms. *Geochimica et Cosmochimica Acta*, 58(19): 4127—4145. doi: 10.1016/0016-7037(94)90269-0
- Wu, F. Y., Li, X. H., Zheng, Y. F., et al., 2007. Lu-Hf Isotopic Systematics and their Applications in Petrology. *Acta Petrologica Sinica*, 23(2): 185—220 (in Chinese with English abstract).
- Wu, C. L., Yang, J. S., Yang, H. Y., et al., 2005. The Zircon SHRIMP Dating and Geological Significance of the two I-type Granites in the Eastern Qilian. *Acta Geologica Sinica*, 20(2): 286 (in Chinese with English Abstract).
- Xia, L. Q., Li, X. M., Yu, J. Y., et al., 2016. Mid-Late Neoproterozoic to Early Paleozoic Volcanism and Tectonic Evolution of the Qilian Mountain. *Geology in China*, 43(4): 1087—1138 (in Chinese with English Abstract).
- Xiao, W. J., Windley, B. F., Yong, Y., et al., 2009. Early Paleozoic to Devonian Multiple-Accretionary Model for the Qilian Shan, NW China. *Journal of Asian Earth Sciences*, 35(3—4): 323—333. doi: 10.1016/j.jseas.2008.10.001
- Xu, J. Q., Li, Z., Shi, Y. H., 2013. Jurassic Detrital Zircon U-Pb and Hf Isotopic Geochronology of Luxi Uplift, Eastern North China, and its Provenance Implications for Tectonic-paleogeographic Reconstruction. *Journal of Asian Earth Sciences*, 78: 184—197. doi: 10.1016/j.jseas.2013.05.024
- Xu, X. Y., Wang, H. L., Chen, J. L., et al., 2008. Zircon U-Pb Dating and Petrogenesis of Xinglongshan Group Basic Volcanic Rocks at Eastern Segment of Middle Qilian Mountains. *Acta Petrologica Sinica*, 24(4): 827—840 (in Chinese with English abstract).
- Xu, X., Song S. G., Su, L., et al., 2015. The 600—580 Ma Continental Rift Basalts in North Qilian Shan, Northwest China: Links between the Qilian-Qaidam Block and SE Australia, and the Reconstruction of East Gondwana. *Precambrian Research*, 257: 47—64. doi: 10.1016/j.precamres.2014.11.017
- Xu, Y. J., Du, Y. S., Yang, J. H., 2013. Tectonic Evolution of the North Qilian Orogenic Belt from the Late Ordovician to Devonian: Evidence from Detrital Zircon Geochronology. *Earth Science*, (5): 934—946 (in Chinese with English abstract).
- Xu, Z. Q., Xu, H. F., Zhang, J. X., et al., 1994. The Zhoulangnanshan Caledonian Subductive Complex in the Northern Qilian Mountains and its Dynamics. *Acta Geologica Sinica*, 68(1): 1—15 (in Chinese with English abstract).
- Xu, W. C., Zhang, H. F., Liu, X. M., 2007. The chronology and Tectonic Significance of the High-grade Metamorphic Rocks of Qilian Mountains: Constraints from Zircon U-Pb Dating. *Chinese Science Bulletin*, 10: 1174—1180 (in Chinese).
- Yang, H., Zhang, H. F., Luo, B. J., et al., 2015. Early Paleozoic Intrusive Rocks from the Eastern Qilian Orogen, NE Tibetan Plateau: Petrogenesis and Tectonic Significance. *Lithos*, 224—225: 13—31. doi: 10.1016/j.lithos.2015.02.020
- Yong, Y., Xiao, W. J., Yuan, C., et al., 2008. Geochronology and Geochemistry of Paleozoic Granitic Plutons From the Eastern Central Qilian and their Tectonic Implications. *Acta Petrologica Sinica*, 24(4): 855—866 (in Chinese with English abstract).
- Yu, S. Y., Zhang, J. X., Real, P. G. D., et al., 2013. The Grenvillian Orogeny in the Altun-Qilian-North Qaidam Mountain Belts of Northern Tibet Plateau: Constraints from Geochemical and Zircon U-Pb Age and Hf Isotopic Study of Magmatic Rocks. *Journal of Asian Earth Sciences*, 73: 372—395. doi: 10.1016/j.jseas.2013.04.042
- Yuan, H. L., Gao, S., Dai, M. N., et al., 2008. Simultaneous Determinations of U-Pb Age, Hf Isotopes and Trace Element Compositions of Zircon by Excimer Laser-Ablation Quadrupole and Multiple-Collector ICP-MS. *Chemical Geology*, 247(1—2): 100—118. doi: 10.1016/j.chemgeo.2007.10.003
- Zhang, B. H., Zhang, J., Zhang, Y. P., et al., 2016. Tectonic Affinity of the Alxa Block, Northwest China: Constrained by Detrital Zircon U-Pb Ages from the Early Paleozoic Strata on its Southern and Eastern Margins. *Sedimentary Geology*, 339: 289—303. doi: 10.1016/j.sedgeo.2016.02.017
- Zhang, C., Bader, T., Zhang, L. F., et al., 2017. The Multi-Stage Tectonic Evolution of the Xitieshan Terrane, North Qaidam Orogen, Western China: From Grenville-Age Orogeny to Early-Paleozoic Ultrahigh-Pressure Metamorphism. *Gondwana Research*, 41: 290—300. doi: 10.1016/j.gr.2015.04.011
- Zhang, J. X., Meng, F. C., Yu, S. Y., 2010. Two Contrasting HP/LT and UHP Metamorphic Belts: Constraint on Early Paleozoic Orogeny in Qilian-Altun Orogen. *Acta Petrologica Sinica*, 26(7): 1967—1992 (in Chinese with English abstract).

- Zhang, J., Zhang, Y.P., Xiao, W.X., et al., 2015. Linking the Alxa Terrane to the Eastern Gondwana during the Early Paleozoic: Constraints from Detrital Zircon U-Pb Ages and Cambrian Sedimentary Records. *Gondwana Research*, 28(3): 1168–1182. doi:10.1016/j.gr.2014.09.012
- Zhang, L.F., Wang, Q.J., Song, S.G., 2009. Lawsonite Blueschist in Northern Qilian, NW China: *P-T* Pseudosections and Petrologic Implications. *Journal of Asian Earth Sciences*, 35(3–4): 354–366. doi:10.1016/j.jseaes.2008.11.007
- Zhang, Q., Sun, X.M., Zhou, D.J., et al., 1997. The Characteristics of North Qilian Ophiolites, Forming Settings and their Tectonic Significance. *Advance in Earth Sciences*, 12(4): 64–91 (in Chinese with English abstract).
- Zhang, Q., Wang, Y., Li, C.D., et al., 2006. Granite Classification on the Basis of Sr and Yb Contents and its Implications. *Acta Petrologica Sinica*, 22(9): 2249–2269 (in Chinese with English abstract).
- Zhang, Q., Wang, Y., Pan, G.Q., et al., 2008. Sources of Granites: Some Crucial Questions on Granite Study (4). *Acta Petrologica Sinica*, 24(6): 1193–1204 (in Chinese with English abstract).
- Zhang, Z.C., Mao, J.W., Yang, J.M., et al., 1998. Geochemical Evidences on the Petrogenesis of the Aoyougou Ophiolite in North Qilian Mountains. *Acta Geologica Sinica*, 72(1): 42–51 (in Chinese with English abstract).
- Zhang, Q., Chen, Y., Zhou, D.J., et al., 1998. The Geochemical Characteristics and Forming Process of the Dachadaban Ophiolite in the North Qilian Mountains. *Sciences in China (Series D)*, 19(1): 30–34 (in Chinese).
- Zhang, Y.J., Sun, F.Y., Xu, C.H., et al., 2016. Geochronology, Geochemistry and Zircon Hf Isotopes of the Tanjianshan Granite Porphyry Intrusion in Dachaidan Area of the North Margin of Qaidam Basin, NW China. *Earth Science*, 41(11): 1830–1844 (in Chinese with English Abstract).
- Zhang, Z.W., Li, W.Y., Wang, Y.L., et al., 2015. Geological and Geochemical Characteristics of Mafic-ultramafic Intrusions in the Hualong Area, Southern Qilian Mountains and Its Ni-Cu Mineralization. *Acta Geologica Sinica*, 89(3): 632–644 (in Chinese with English Abstract).
- Zorpi, M.J., Coulon, C., Orsini, J.B., et al., 1989. Magma Mingling, Zoning and Emplacement in Calc-Alkaline Granitoid Plutons. *Tectonophysics*, 157(4): 315–329. doi:10.1016/0040-1951(89)90147-9
- Zuo, G.C., Liu, J.C., 1987. The Evolution of Tectonic of Early Paleozoic in North Qilian Range, China. *Chinese Journal of Geology*, 22(1): 14–24 (in Chinese with English abstract).
- 附中文参考文献**
- 陈加杰, 付乐兵, 魏俊浩, 等, 2016. 东昆仑沟里地区晚奥陶世花岗闪长岩地球化学特征及其对原特提斯洋演化的制约. *地球科学*, 41(11): 1863–1882.
- 第五春荣, 孙勇, 王倩, 2012. 华北克拉通地壳生长和演化: 来自现代河流碎屑锆石 Hf 同位素组成的启示. *岩石学报*, 28(11): 3520–3530.
- 董国安, 杨怀仁, 杨宏仪, 等, 2007. 祁连地块前寒武纪基底锆石 SHRIMP U-Pb 年代学及其地质意义. *科学通报*, 52(13): 1572–1585.
- 杜德道, 曲晓明, 王根厚, 等, 2011. 西藏班公湖—怒江缝合带西段中特提斯洋盆的双向俯冲: 来自岛弧型花岗岩锆石 U-Pb 年龄和元素地球化学的证据. *岩石学报*, 27(7): 1993–2002.
- 杜远生, 朱杰, 顾松竹, 等, 2006. 北祁连造山带寒武系—奥陶系硅质岩沉积地球化学特征及其多岛洋构造意义. *地球科学*, 31(1): 101–109.
- 冯益民, 何世平, 1995. 北祁连蛇绿岩的地质地球化学研究. *岩石学报*, 11(S1): 125–140+142–146.
- 冯益民, 何世平, 1996. 祁连山大地构造与造山作用. 北京: 地质出版社.
- 冯益民, 1997. 祁连造山带研究概况——历史、现状及展望. *地球科学进展*, 12(4): 5–12.
- 关俊雷, 耿全如, 彭智敏, 等, 2016. 西藏唐古拉岩岩浆岩带夏马日花岗岩体的岩石学、岩石地球化学、锆石 U-Pb 测年及 Hf 同位素组成. *地质学报*, 90(2): 304–333.
- 郭进京, 张国伟, 陆松年, 等, 1999. 中祁连地块东段元古宙基底地层格架讨论. *中国区域地质*, 18(4): 379–382.
- 郭进京, 赵凤清, 李怀坤, 等, 2000. 中祁连东段涅源群的年代学新证据及其地质意义. *中国区域地质*, 19(1): 26–31.
- 郭原生, 孙淑荣, 傅学明, 1993. 北祁连西段蛇绿岩型超基性岩微量元素特征及其地质意义. *兰州大学学报*, (3): 206–212.
- 侯可军, 李延河, 田有荣, 2009. LA-MC-ICP-MS 锆石微区原位 U-Pb 定年技术. *矿床地质*, 28(4): 481–492.
- 黄增保, 郑建平, 李葆华, 等, 2016. 南祁连大道尔吉早古生代弧后盆地型蛇绿岩的年代学、地球化学特征及意义. *大地构造与成矿学*, 40(4): 826–838.
- 姜高磊, 张思敏, 柳坤峰, 等, 2014. 祁连—柴达木—东昆仑新元古—中生代沉积盆地演化. *地球科学*, (8): 1000–1016.
- 李昌年, 1992. 火成岩微量元素岩石学. 武汉: 中国地质大学出版社.
- 李建锋, 张志诚, 韩宝福, 2010. 中祁连西段肃北、石包城地区早古生代花岗岩年代学、地球化学特征及其地质意义. *岩石学报*, 26(8): 2431–2444.
- 李兆, 陈岳龙, 刘长征, 等, 2016. 北祁连的形成与演化历史:

- 来自河流沉积物地球化学及其碎屑锆石 U-Pb 年龄、Hf 同位素组成的证据.地质学报,90(2): 267-283.
- 刘颖,刘海臣,李献华,1996.用 ICP-MS 准确测定岩石样品中的 40 余种微量元素.地球化学,25(6): 552-558.
- 裴先治,李佐臣,李瑞保,等,2012.祁连造山带东段早古生代葫芦河群变质碎屑岩中碎屑锆石 LA-ICP-MSU-Pb 年龄:源区特征和沉积时代的限定.地学前缘,19(5): 205-224.
- 钱家骥,宫保军,窦尚仁,等,1986.中祁连山西段元古界的叠层石研究.甘肃地质,(0): 1-32+147-160.
- 钱青,孙晓猛,张旗,等,1999.北祁连九个泉蛇绿岩及其上覆岩系的岩石地球化学特征和地球动力学意义.地质论评,45(S1): 1038-1046.
- 青海省地矿局,1991.青海省区域地质志.北京:地质出版社.
- 秦海鹏,吴才来,王次松,等,2014a.北祁连下古城花岗岩体 LA-ICP-MS 锆石 U-Pb 年代学及岩石化学特征.地质学报,88(10): 1832-1842.
- 秦海鹏,吴才来,王次松,等,2014b.祁连东部西格拉高 Sr/Y 型花岗岩 LA-ICP-MS 锆石 U-Pb 定年及其地球化学特征.岩石学报,30(12): 3759-3771.
- 邱检生,肖娥,胡建,等,2008.福建北东沿海高分异 I 型花岗岩的成因:锆石 U-Pb 年代学、地球化学和 Nd-Hf 同位素制约.岩石学报,24(11): 2468-2484.
- 宋述光,张贵宾,张聪,等,2013.大洋俯冲和大陆碰撞的动力学过程:北祁连—柴北缘高压—超高压变质带的岩石学制约.科学通报,58(23): 2240-2245.
- 万渝生,许志琴,杨经绥,等,2003.祁连造山带及邻区前寒武纪深变质基底的时代和组成.地球学报,24(4): 319-324.
- 王洪亮,何世平,陈隽璐,等,2007.甘肃马衔山花岗岩杂岩体 LA-ICPMS 锆石 U-Pb 测年及其构造意义.地质学报,81(1): 72-78.
- 吴才来,杨经绥,杨宏仪,等,2005.北祁连东部两类 I 型花岗岩定年及其地质意义.地质学报,79(2): 286.
- 吴福元,李献华,郑永飞,等,2007.Lu-Hf 同位素体系及其岩石学应用.岩石学报,23(2): 185-220.
- 夏林圻,李向民,余吉远,等,2016.祁连山新元古代中—晚期至早古生代火山作用与构造演化.中国地质,43(4): 1087-1138.
- 徐旺春,张宏飞,柳小明,2007.锆石 U-Pb 定年限制祁连山高级变质岩系的形成时代及其构造意义.科学通报,52(10): 1174-1180.
- 徐学义,王洪亮,陈隽璐,等,2008.中祁连东段兴隆山群基性火山岩锆石 U-Pb 定年及岩石成因研究.岩石学报,24(4): 827-840.
- 徐亚军,杜远生,杨江海,2013.北祁连造山带晚奥陶世—泥盆纪构造演化:碎屑锆石年代学证据.地球科学,(5): 934-946.
- 许志琴,徐惠芬,张建新,等,1994.北祁连走廊南山加里东俯冲杂岩增生地体及其动力学.地质学报,68(1): 1-15.
- 雍拥,肖文交,袁超,等,2008.中祁连东段古生代花岗岩的年代学、地球化学特征及其大地构造意义.岩石学报,24(4): 855-866.
- 张建新,孟繁聪,于胜尧,2010.两条不同类型的 HP/LT 和 UHP 变质带对祁连—阿尔金早古生代造山作用的制约.岩石学报,26(7): 1967-1992.
- 张旗,Chen, Y.,周德进,等,1998.北祁连大岔蛇绿岩的地球化学特征及其成因.中国科学:D 辑:地球科学,(1): 30-34.
- 张旗,孙晓猛,周德进,等,1997.北祁连蛇绿岩的特征、形成环境及其构造意义.地球科学进展,12(4): 64-91.
- 张旗,王焰,李承东,等,2006.花岗岩的 Sr-Yb 分类及其地质意义.岩石学报,22(9): 2249-2269.
- 张旗,王焰,潘国强,等,2008.花岗岩源岩问题——关于花岗岩研究的思考之四.岩石学报,24(6): 1193-1204.
- 张延军,孙丰月,许成瀚,等,2016.柴北缘大柴旦滩间山花岗岩斑岩体锆石 U-Pb 年代学、地球化学及 Hf 同位素.地球科学,41(11): 1830-1844.
- 张招崇,毛景文,杨建民,等,1998.北祁连熬油沟蛇绿岩岩石成因的地球化学证据.地质学报,72(1): 42-51.
- 张照伟,李文渊,王亚磊,等,2015.南祁连化隆地区镁铁—超镁铁质侵入岩地质、地球化学特征与铜镍成矿.地质学报,89(3): 632-644.
- 左国朝,刘寄陈,1987.北祁连早古生代大地构造演化.地质科学,22(1): 14-24.